DEVELOPMENT AND TESTING OF PULSED PLASMA THRUSTER

A PROJECT REPORT

Submitted by

ALDRIN INBARAJ A (18103066)

KAMALESH T (18103052)

MEET BHANUSHALI (18103013)

In partial fulfilment for the award of the degree

of

BACHELOR OF TECHNOLOGY

IN

AEROSPACE ENGINEERING

SCHOOL OF AERONAUTICAL SCIENCES

HINDUSTAN INSTITUTE OF TECHNOLOGY AND SCIENCE

PADUR, CHENNAI - 603 103

MAY 2022

HINDUSTAN INSTITUTE OF TECHNOLOGY AND SCIENCE
PADUR, CHENNAI - 603 103

BONAFIDE CERTIFICATE

Certified that this project report titled **"DEVELOPMENT AND TESTING OF PULSED PLASMA THRUSTER"** is the bonafide work of **"ALDRIN INBARAJ A (18103066), KAMALESH T (18103052), MEET BHANUSHALI (18103013)"** who carried out the project work under my supervision. Certified further that to the best of my knowledge the work reported here does not form part of any other project / research work on the basis of which a degree or award was conferred on an earlier occasion on this or any other candidate.

HEAD OF THE DEPARTMENT	**SUPERVISOR**
Dr. P. Vasantha Kumar	**Mr. G. Dinesh Kumar**
Professor	Assistant Professor
Department of Aerospace Engineering Hindustan Institute of Technology & Science Padur	Department of Aeronautical Engineering Hindustan Institute of Technology & Science Padur

The Project Viva-Voce examination is held on _______________

INTERNAL EXAMINER	**EXTERNAL EXAMINER**

ACKNOWLEDGEMENT

We would like to place on record our sincere thanks to all those who contributed to the successful completion of our final year project work.

It's a matter of pride and privilege for us to express our deep gratitude to the management of Hindustan Institute of Technology and Science for providing us with the necessary facilities and support.

We express our deep sense of gratitude to our respected Chairperson **Dr. (Mrs.) Elizabeth Verghese** and Pro-Chancellor **Dr. Anand Jacob Verghese** for giving us an opportunity to do the project.

We would like to thank our Director **Mr. Ashok Verghese** and Vice-Chancellor **Dr. S.N. Sridhara** for giving us moral support to complete this project.

We would like to express our grateful thanks to Dean (E&T)) **Dr. Angellina Geetha** and Registrar **Dr. Pon. Ramalingam** for support and encouragement.

We extend our sincere thanks to our Head of the Department **Dr.R. Asokan,** Head of Aeronautical Engineering and **Dr.P. Vasanthakumar,** Head of Aerospace Engineering for inspiring and motivating us to complete this project.

We would like to thank our guide **Mr. Dinesh Kumar G** for continually guiding and actively participating in our project, giving valuable suggestion to complete our project.

We would like to thank all the faculty members of the School of Aeronautical Sciences, who have directly or indirectly extended their support.

Last, but not least, we are deeply indebted to our parents who have been our greatest support while we worked day and night to make the project a success.

ABSTRACT

Pulsed plasma thrusters are low-power electric thrusters with high-specific-impulse. They use solid propellants which reduce the hassle of complex designs for valves and chambers and weigh relatively very lower compared to any other thrusters. Used mainly in Cubesats, they are capable of performing orbit maneuvers, attitude control, station keeping and enable deep space missions.

In this paper we elaborately discuss ways of fabricating a Pulsed plasma thrusters with low cost alternatives including trade and selection of electrode materials, fuel, dc power source, capacitors and drivers. Ways to measure high voltage easily and manufacturing an optimal vacuum chamber are also discussed in this paper. Flyback Transformer is used as primary DC power source with ballasts to drive them. Capacitors are charged up using the given voltage and discharged by inducing a spark across the plates. As an arc is formed between the two plates, PTFE (Teflon) gets ablated and produces plasma which is expelled as an impulse bit. Characteristics of the pulsed plasma thruster is studied based on the results from testing the setup under vacuum.

Keywords

Pulsed plasma thruster, Cubesats, Electric propulsion, Flyback Transformer, PTFE, Impulse bit

TABLE OF CONTENTS

LIST OF TABLES

LIST OF FIGURES

LIST OF SYMBOLS AND ABBREVIATION

LIST OF SYMBOLS	
j	Current
B	Induced Magnetic field
V_{in}	Input voltage
V_{out}	Output voltage
R_1	Resistance of resistor 1
R_2	Resistance of resistor 2
I_{bit}	Impulse bit
m	Mass of pendulum
g	Acceleration due to gravity
L	Length of pendulum
x	Displacement of pendulum
F	Force
Δt	Discharge time
θ	Angle displaced by the pendulum

LIST OF ABBREVATIONS	
TRL	Technology readiness level
NASA	National Aeronautics and Space Administration
PPT	Pulsed Plasma thruster
PTFE	polytetrafluoroethylene
SMS	Synchronous Meteorological Satellite
LPPT	Liquid pulsed plasma thruster
ZVS	Zero voltage switching

VVS	Valley Voltage Switching
ESU	energy storage unit
AC	Alternating current
DC	Direct current
CW	Cockroft Walton
MOSFET	Metal oxide semiconductor field effect transistor
IGBT	Insulated gate bipolar transistor
LED	Light emitting diode
PLA	Polylactic Acid
AWG	American Wire Gauge
RTV	Room temperature vulcanizing silicone
LOT/LOPT	Line output transformer
NC	Normally closed
AIS	Applied Ion Systems

CHAPTER 1

INTRODUCTION

In-space small spacecraft propulsion technologies are generally categorized as (i) chemical, (ii) electric, or (iii) propellant-less.

Pulsed plasma thrusters come under electric thrusters and are one of the most used type of thruster for propelling spacecrafts in space with a TRL of 9. They are used widely due to their simplicity and compact design in terms of fuel storage and space required for the mechanism compared to chemical or liquid engines which require chambers and valves for operating. They also provide high specific impulse compared to solid motors as shown in Figure 1.1.

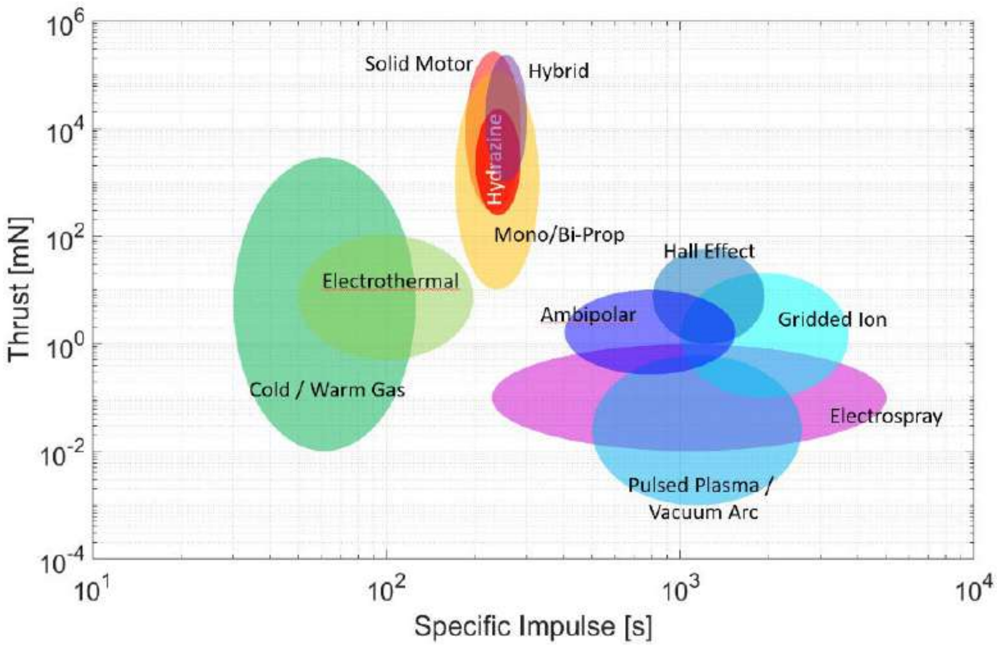

Fig 1.1 *Specific impulse vs Thrust for various propulsion systems. Credits - NASA*

Table 1.1 displays all the technologies currently available and tested for a comparison. As we can see from the table, pulsed plasma thruster is up in the place among the top thrusters with high specific impulse.

Table 1.1 Summary of Propulsion Technologies Surveyed.

Credits - NASA

Technology	Thrust Range	Specific Impulse Range [sec]
CHEMICAL PROPULSION TECHNOLOGIES		
Hydrazine Monopropellant	0.25 – 25 N	200 – 285
Alternative Mono- and Bipropellants	10 mN – 120 N	160 – 310
Hybrids	1 – 230 N	215 – 300
Cold / Warm Gas	10 μN – 3 N	30 – 110
Solid Motors	0.3 – 260 N	180 – 280
Propellant Management Devices	N/A	N/A
ELECTRIC PROPULSION TECHNOLOGIES		
Electrothermal	0.5 – 100 mN	50 – 185
Electrosprays	10 μN – 1 mN	225 – 5,000
Gridded Ion	0.1 – 20 mN	1,000 – 3,500
Hall-Effect	1 – 60 mN	800 – 1,950
Pulsed Plasma and Vacuum Arc Thrusters	1 – 600 μN	500 – 2,400
Ambipolar	0.25 – 10 mN	400 – 1,400
PROPELLANTLESS PROPULSION TECHNOLOGIES		
Solar Sails	TBD	N/A
Electrodynamic Tethers	TBD	N/A
Aerodynamic Drag	TBD	N/A

Pulsed Plasma Thrusters (PPT) produce thrust by first triggering an electric arc between a pair of electrodes that typically ablates a solid-state propellant like polytetrafluoroethylene (PTFE) or ionizes a gaseous propellant. The plasma is accelerated by an induced electromagnetic field due to flow of current from anode to cathode.

Electrothermal PPTs characteristically include a chamber formed by a pair of electrodes and solid propellant, wherein propellant ablation and heating occurs. During and immediately following each electric discharge, pressure accumulates and accelerates the propellant through a single opening. Electromagnetic PPTs characteristically do not highly confine the propellant as plasma forms. The current pulse, which may exceed tens of thousands of amps, highly ionizes the ablated material or gas. The current pulse further establishes a magnetic field, where the **jxB** force accelerates the plasma. PPT devices that are predominantly electrothermal typically offer higher thrust, while devices that are predominantly electromagnetic offer higher specific impulse.

PPT devices are suitable for attitude control and precision pointing applications. PPTs offer small and repeatable impulse bits, which allow for very high precision maneuvering. The complete propulsion system consists of a thruster, an ignitor, and a power processing unit (PPU). Energy to form the pulsed discharge is stored in a high voltage capacitor bank, which often accounts for a significant portion of the system mass. Once the capacitors are charged, resulting in a large differential voltage between the electrodes, the ignitor provides seed material that allows the discharge between the electrodes to form. Various materials and gases (including water vapor) have been tested with PPTs, however PTFE remains most common.

CHAPTER 2
LITERATURE REVIEW

2.1 PULSED PLASMA THRUSTERS HISTORY

On Nov. 30, 1964, the Zond 2 spacecraft was launched toward Mars from Baikonur in the Soviet Union. Several months later, radio communication was lost, and with it control of the electric propulsion system designed to provide three axis attitude control. The Zond 2 pulsed plasma thrusters (PPTs) were the first application of electric propulsion on any spacecraft. Other successful flight applications of the PPT followed in the United States. In 1968 a PPT on the LES-6 satellite began 10 years of service providing attitude control. In 1974 a PPT was deployed on the Synchronous Meteorological Satellite (SMS). And beginning in 1981 the Navy TRANSIT navigation satellite system employed three spacecraft called the TIP/NOVA (TRANSIT Improvement Program) series, which used PPTs for drag makeup to maintain a ‘‘drag-free’’ orbital position. These spacecraft accumulated a total of 28 thruster years of successful operation.

Table 2.1 Thrust and mass ablation characteristics of various PPTs [1]

Thruster	E_O, J	Type	I_{sp}, s	I_{bit}, μN-s	I_{bit}/J, μN-s/J	$\Delta m/E_O$, μg/J	Δm/area, μg/cm^2
LES-6	1.85	Breech-fed	300	26	14	4.8	3.3
SMS	8.4	Breech-fed	450	133	15	3.4	3.9
LES-8/9	20	Breech-fed	1000	297	15	1.5	4.8
TIP-II(NOVA)	20	Breech-fed	850	375	19	2.3	5.7
MIT Lab	20	Side-fed	600	454	23	2.8	4.3
MIPD-3	100	Side-fed	1130	2250	23	2.0	4.3
Millipound	750	Side-fed	1210	22,300	30	2.5	27.7
Primex-NASA	43	Breech-fed	1136	737	17	1.5	2.6
IL PPT-3 Lab	7.5	Coax-side-fed	600	450	60	10.0	36.0
Japan Lab	30.4	Breech-fed	423	469	15	3.7	6.4
China Lab	23.9	Breech-fed	990	448	19	1.9	5.3

2.2 PROPELLANTS USED

PTFE eliminates the need for common storage tanks and propellant supply lines and valves. However, due to the self-adjusting supply of mass and power, PPT propellant utilization and thrust efficiency are low. All three state of matter propellants have been analyzed for PPT. However, PTFE has always been the best propellant for space applications. [2]

Table 2.2 PPT alternative propellants used so far.

State	Alternative propellants
Solid	Fluorocarbons, Teflon sintered, seeded or impregnated Teflon, composite propellants, powdered propellants
Gas	Argon, nitrogen, xenon, water vapor
Liquid	Water, methanol, ethanol, buthanol, dimethyl ether (DME), mercury, gallium, lithium, cesium

Solid propellants are generally the preferred propellants because they maintain the simplicity of the system by eliminating the use of storage tanks, supply lines, and valves. High reliability is obtained. Solid propellants studied so far include a variety of fluorocarbons and composites.

Among the gaseous fuels studied, argon, xenon, nitrogen and water vapor can be mentioned. This resulted in high specific impulse and thrust efficiency at very high operating frequencies above 1 kHz. Over the years, water, methanol, ethanol, butanol, DME, mercury, gallium, lithium, and cesium have been studied numerically or experimentally. High specific impulse and thrust efficiency, and low momentum to energy ratio were typical properties of liquid propellants for PPT.

Teflon seeded and sintered with 10% and 30% of LiOH and InBr were investigated and the results were no higher than PTFE. However, a constant decrease in impulse bit was experienced for both sintered cases when number of
pulses increased.

Liquid and gaseous propellants were promising because they allowed the independent input of mass and energy into the PPT. Higher molecular weight propellants result in higher exhaust velocities, higher specific impulses, and higher thrust efficiencies. Water has a lower average molecular weight and higher specific impulse than PTFE. From the experimental results, it was reported that water LPPT has high specific impulse, thrust efficiency, and propellant utilization efficiency, but the momentum-to-bit and momentum-to-energy ratios of water LPPT and PTFE are low.

Argon provided higher specific impulse and thrust efficiency, and an impulse bit comparable to xenon, at the same energy level and mass shot. Their performance data on lower mass shots showed higher specific impulse and thrust efficiency, but lower impulse bits compared to PTFE.

Water vapor is used in rectangular PPTs, providing the highest performance parameters of any other gas propellant, and the results certify it as a viable propellant option for GPPT. Preliminary results of combining solid propellant and liquid propellant into one discharge show an expected increase in impulse bit, but has deficiencies regarding specific impulse and thrust efficiency as a result of the elevated mass.

A qualitative comparison of investigated PPT alternative propellant is provided below

Table 2.3 Comparison of PPT alternative propellants.

Propellant	Advantages	Disadvantages
Solid		
PTFE	No valves, injectors, and feed control, easy storage and handling, abundant, high I/E	Low I_{sp}, late-time ablation, particulate emission, coupled mass and energy feed
Fluorocarbons		
Teflon sintered, seeded or impregnated Teflon		
composite propellants		
powdered propellants		
Liquid		
Water	Independent mass and energy feed, abundant, high I_{sp}	Need for valve, injector, and storage, low I/E, low degree of ionization, heater needed (additional mass and power), Leakage
DME		
Methanol		
Gaseous		
Xenon	Independent mass and energy feed, high I_{sp}, high I/E at medium and high power, precise mass feed and control	Rare, need for fast-acting valve, injector, and high-pressure storage, low I/E at low power
Argon	Independent mass and energy feed, abundant, high I_{sp}, precise mass feed and control	Very high pulse frequency for good operation, leakage, need for fast-acting valve, injector, and high-pressure storage, low I/E
Nitrogen		
Water vapor		

2.3 PRIOR WORKS

Anuscheh Nawaz *et al* (2008) investigates the role of magnetic field which is induced due to flow of currents through electrodes. The current through the plasma interacts with the circuit's own magnetic field, causing an electromagnetic force on the plasma sheet along the electrodes. As a result of this Lorentz force, the current sheet is expelled from the thrusters exhaust. The magnetic field was measured by using an induction coil. Magnetic field measurements were conducted in a cylindric vacuum chamber, at base pressures of $2 x 10^4$ mbar. The magnetic field probe was attached to a two-axis table, installed in front of the thruster's exhaust. The magnetic field was calculated between the electrodes using the law of Biot–Savart. [3]

Simone Ciaralli (2014) discusses in detail about working of various pulsed plasma thrusters and their lifetime. He also discusses the problem faced that cause shorter lifetime and fabricates another pulsed plasma thruster to solve the stated issues. [4]

Kateryna Aheieva *et al* (2015) gives a very simple and efficient way to measure impulse bit of any electric thruster by using a pendulum system which is discussed in detail in Chapter 6. He also states that by using a magnet to increase the speed at which plasma is expelled out, we can increase the impulse bit by 30% as far as Vacuum arc thruster is concerned. [5]

Kang Bingyin (2017) talks in detail about methods to use flyback transformer efficiently using ZVS drivers. A flyback circuit was proposed for a PPT igniter. Unlike other topologies that require physical high voltage capacitors, this topology uses the parasitic capacitances of transformer, MOSFET, diode and igniter spark plugs. Hence, the reliability of PPT igniter is improved by avoiding the capacitor failure probability of 13.4%. To overcome the drawbacks of hard-switching technique, he also proposes a quasi-resonant DC-DC converter for a PPT igniter. Two switching control approaches have been discussed. One is zero-voltage-switching (ZVS) used throughout the charging process. The other one is hybrid switching including valley-voltage-switching (VVS) in the first few charging cycles and ZVS in the remaining cycles. [6]

Aditya R. Khuller *et al* (2018) developed a pulsed plasma thruster as a student project from Arizona State University. In their paper, they exaplain about all the components used in their thruster. Their work will cover the design and development of a multi-axis PPT module with a compact form factor of 0.9U and a maximum mass of about 1kg, minimizing the volume and mass of the system and enabling larger scientific payloads increase. [7]

CHAPTER 3

METHODOLOGY

3.1 GENERAL PPT OVERVIEW

The PPT contains two electrodes positioned close to the propellant source. An energy storage unit (ESU) or capacitor placed in parallel with the electrodes is charged to a high voltage by the thruster's power supply. The first step for initiating a PPT pulse is ignition. The thruster's igniter, mounted close to the propellant, produces a spark that allows a discharge of the ESU between the electrodes to create a plasma. This plasma is called the main discharge. The main discharge ablates and ionizes the surface portion of the solid propellant, creating a propellant plasma. This plasma is then accelerated out of the thruster by the Lorentz force. The Lorentz force is a force created by the interaction of a magnetic field and an electric current. As the propellant is consumed, a spring forces the remaining solid propellant forward, providing a constant fuel source. Credits - NASA

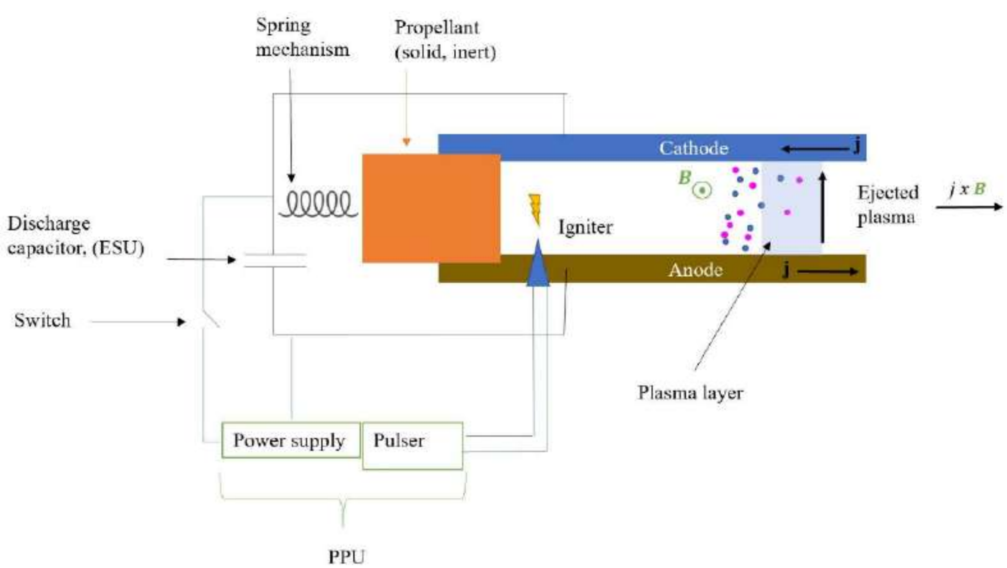

Figure 3.1 *PPT working principle [8]*

3.2 ABLATION MODEL

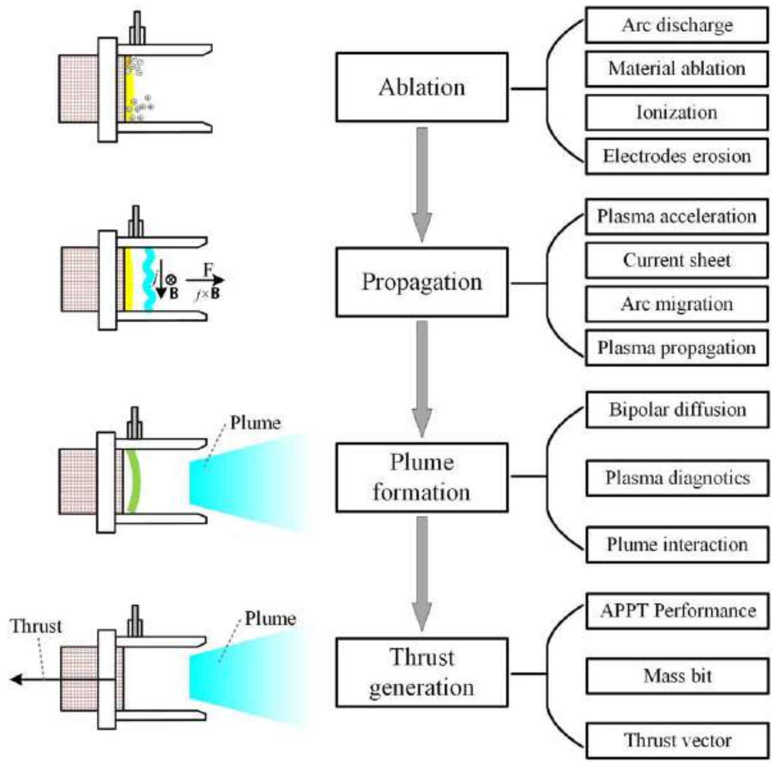

Figure 3.2 *Ablation process of Teflon [9]*

The events that take place from charging up the capacitors to getting one impulse bit from the thruster is explain in Figure 3.2.

In the first process, an arc forms as we charge up the capacitors connecting cathode and anode plates of the thruster and a spark is induced through a spark igniter. The arc formed due to coronal discharge across plates due to high voltage.

Next, current flows from cathode to anode and thereby induces a magnetic field due to Lorentz force. Force generated perpendicular to magnetic field and current flow pushes the spacecraft forward. The plume is essentially accelerated due to the magnetic field during this process. The impulse bit thus generated is measured using a thrust measurement system and the performance of the thruster is determined.

CHAPTER 4
COMPONENTS SELECTION

4.1 PLATE MATERIAL

Cathode and anode of the thruster are made up of conducting materials like copper or aluminium and the tradeoff between them is given below.

4.1.1 ALUMINIUM PLATE

Though it has only 30 percent of the weight of copper, it has only 61% of the conductivity of copper. Aluminium corrodes easily, which could cause excessive resistance and heat buildup at connection points

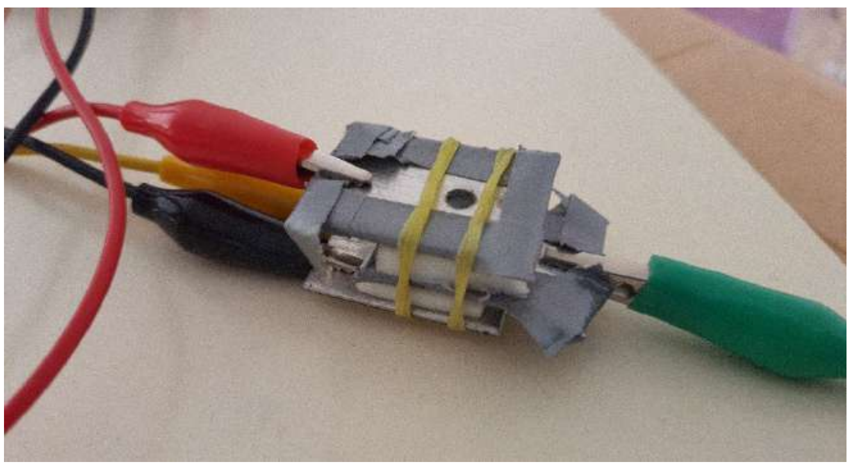

Figure 4.1.1.1 *Aluminium plates stacked*

4.1.2 COPPER PLATE

The two metals are close on the scale of conductivity, with copper having the more desirable characteristic. The conductivity of copper is about 0.6 x 10^6 mho/cm while that of aluminum is about 0.4 x 10^6 mho/cm. Copper wiring has a lower thermal expansion. This means it doesn’t expand as much as aluminum wiring when exposed to heat. Copper's tensile strength is about 40 percent better than that of aluminum and thus copper is less likely to break. Copper plates are thus selected as power plates for the project.

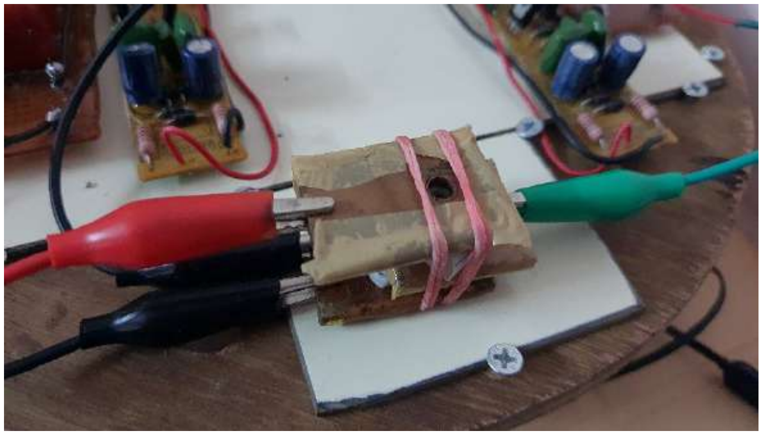

Figure 4.1.2.1 *Copper plates stacked*

4.2 FUEL

4.2.1 TEFLON

Most of the pulsed plasma thrusters use solid polytetrafluoroethylene (PTFE) as a propellant. PTFE is attractive due to its performance in PPTs, ease of storage, and the lack of a need for valves, injectors, heaters, etc. Even if we discount its specific impulse advantage when compared with chemical propulsion, its simplicity still makes it attractive for micro propulsion applications. Conversely, the primary drawbacks of PTFE are the need for a mechanical propellant feeding system (which may become significantly complex for higher propellant masses), carbon deposition on the propellant surface leading to thruster failure, and late-time ablation resulting in particulate emission and a decrease in the propellant utilization efficiency. [10]

4.2.2 OTHER POSSIBLE MATERIALS THAT CAN BE USED

Reducing molecular weight, specific impulse can be increased.

Table 4.2.2.1 PPT alternative propellants [2]

State	Alternative propellants
Solid	Fluorocarbons, Teflon sintered, seeded or impregnated Teflon, composite propellants, powdered propellants

Gas	Argon, nitrogen, xenon, water vapor
Liquid	Water, methanol, ethanol, buthanol, dimethyl ether (DME), mercury, gallium, lithium, cesium

4.3 DC POWER SOURCE

High voltage DC power sources are hard to come by and could cause serious injuries if not handled properly. Given below are some of the converters and transformers used to create high voltage.

4.3.1 FLYBACK TRANSFORMER

A flyback transformer is a coupled inductor with a gapped core. During each cycle, when the input voltage is applied to the primary winding, energy is stored in the gap of the core. It is then transferred to the secondary winding to provide energy to the load.

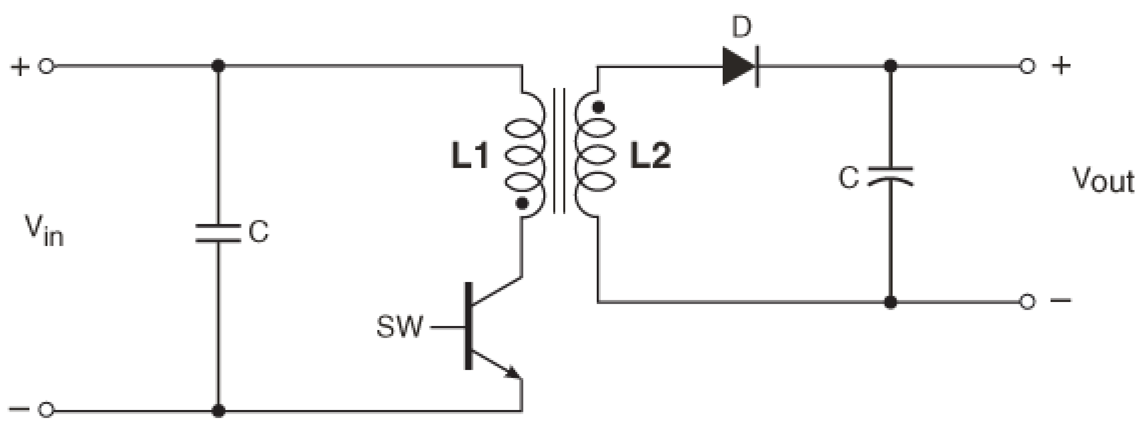

Figure 4.3.1.1 *Flyback transformer schematic*

Traditional transformers are known for stepping up or stepping down AC voltage. The output of the flyback transformer on the other hand is rectified using diodes to give out DC output. For finding the negative pin out of all the pins in the transformer, resistance between any two pins are found. The lowest resistance between two pins are the pins corresponding to the primary coil winding. High frequency AC or pulsed DC is then supplied to these pins to get high voltage output from the long red wire. When the high voltage wire is brought close to the pins in the bottom, one of the pins will complete the circuit and an arc will be produced across these two pins. The other pin is inferred to be the ground pin.

Figure 4.3.1.2 *Flyback Transformer*

4.3.2 COCKROFT WALTON MULTIPLIER

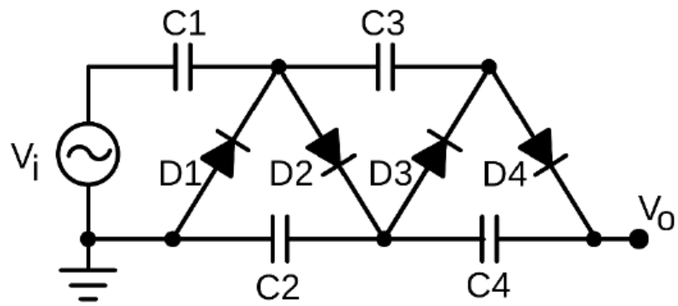

Figure 4.3.2.1 *Two staged Cockroft Walton multiplier*

The Cockcroft-Walton (CW) is a voltage multiplier that converts AC or pulsing DC electrical power from a low voltage level to a higher DC voltage level. A network of capacitors and diodes are used to generate high voltage. In this method, heavy core requirement is eliminated which would be required if transformers are used for the same purpose. The biggest advantage of such circuits is that the voltage across each stage of the cascade is equal to only twice the peak input voltage in a half wave rectifier. In a full wave rectifier it is three times the input voltage.

Considering the simple two-stage version Figure 4.3.2.1 at the time when the AC input reaches its -ve pole the left-most diode is allowing current to flow from the ground into the first capacitor, filling it up. When the same AC signal reverses polarity, current flows through the second diode filling up the second capacitor with both the +ve end from AC source and the first capacitor charging the second capacitor to twice the charge held in the first. With each change in polarity of the input, the capacitors add to the upstream charge and boost the voltage level of the capacitors downstream, towards the output on the right. The increase in voltage, assuming perfect conditions, is twice the input voltage times the number of stages in the multiplier.

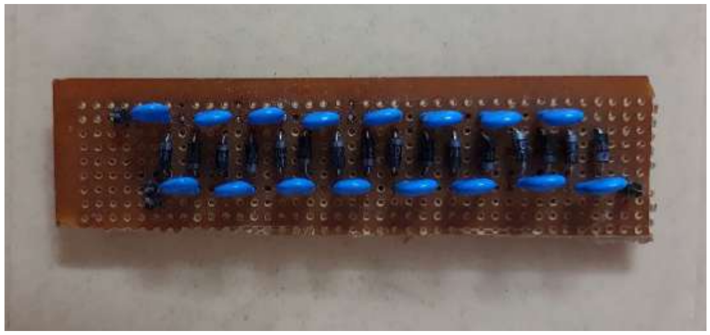

Figure 4.3.2.2 *Eight staged Cockroft Walton multiplier*

Figure 4.3.2.2 is a multiplier custom designed by the team but didn't work as expected due to poor selection of capacitors and diodes.

4.3.3 MARX GENERATOR

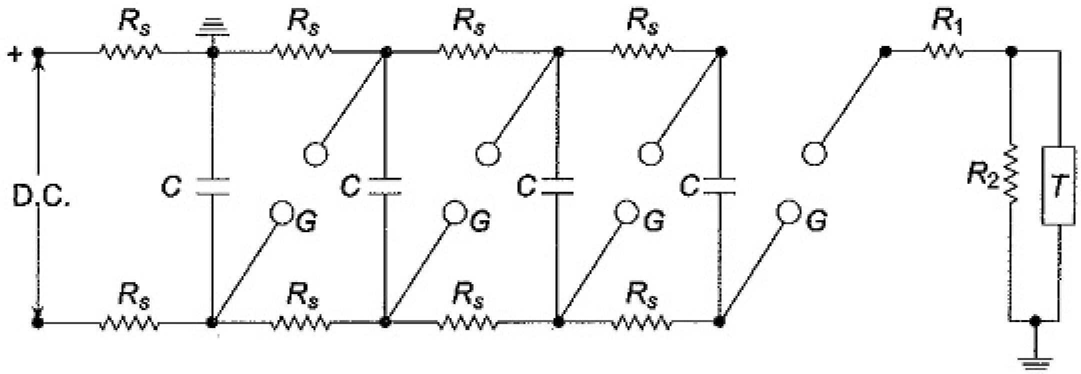

Fig 4.3.3.1 *Conventional Marx generator schematic [11]*

The basic concept of the Marx Generator is that the capacitors are charged in parallel as much as their input DC voltage stage. Those capacitors are then related in series to the use of switches to produce an excessive voltage pulse throughout the circuit. Marx Generator use sparks gas switches. These switches possess barriers like short lifestyle time in terms of several operation cycles, low switching frequency, huge length, extra maintenance, and many others.

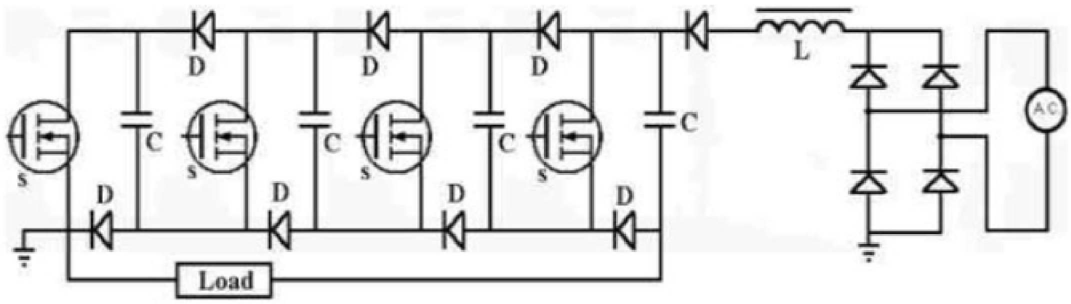

Fig 4.3.3.2 *Modern Marx generator schematic [12]*

Currently, solid state relays like MOSFET or IGBT are used in place of spark gas switches. The benefits of using these are compact design, reliable, bendy, more efficient, long lifestyles time, low charges, and reduced losses. The output pulse width and amplitude each can be varied by controlling the gate control pulses to the switches.

The system includes 4 stages such that each stage is made up of diodes, one MOSFET in conjunction with one capacitor. Diodes are used for capacitor charging at every stage and MOSFET is used as a transfer to keep away from power losses. The capacitors are charged in parallel. When the capacitor has suitable charge saved in it, switches are used to attach all capacitors in series, and the capacitor discharges. We finally get n times of rectifier voltage across the burden.

4.3.4 STEP UP POWER MODULE

Figure 4.3.4.1 *Step Up Power Module*

The module is a combination of mini flyback transformer, diodes, transistors and capacitors immersed in epoxy to avoid internal arcing. A youtuber reverse engineered the components inside the module as shown in Figure 4.3.4.2

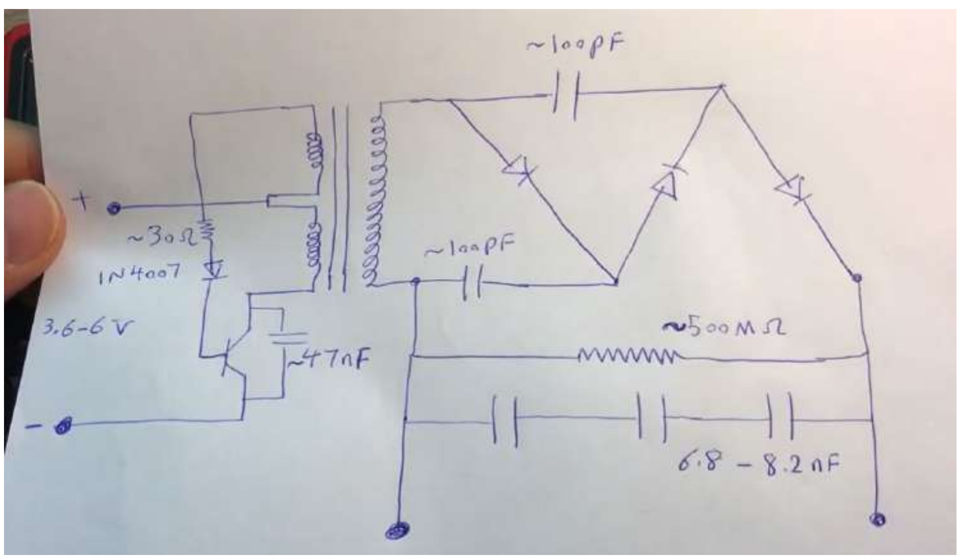

Figure 4.3.4.2 *Step Up Power Module Schematic [https://youtu.be/mTx8pMHo4jI]*

Specifications of the module-

Input voltage (DC) – 3.6 to 6 V

Input current – 2A to 5A

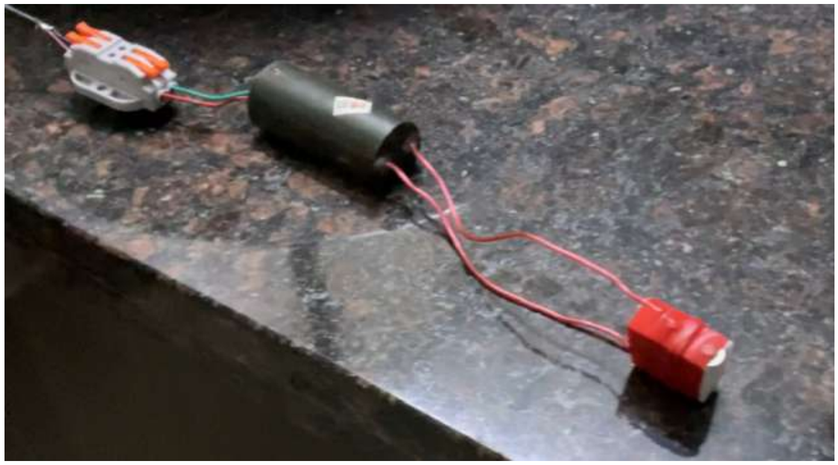

Figure 4.3.4.3 *Step up power module setup*

The module was powered using mobile phone charger adapater which outputs 5v at 2 amps and the results are shown in Figure 4.3.4.4.

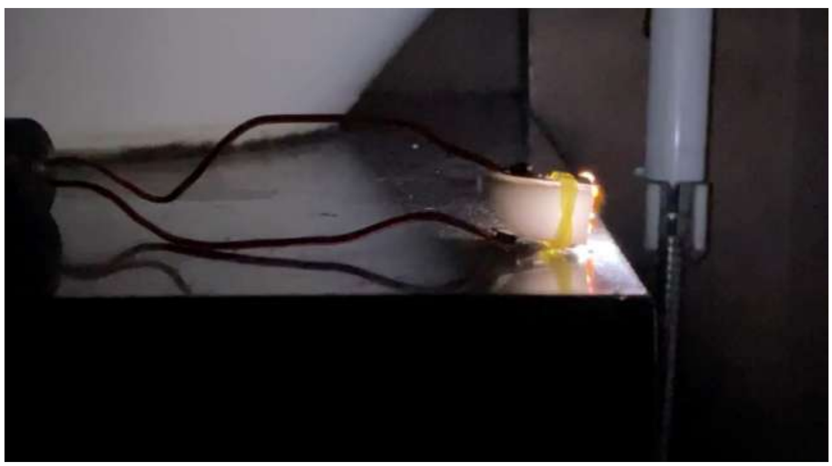

Figure 4.3.4.4 *Teflon Ablating*

Though the Teflon got ablated, there were no control over the discharge because they were pulsed DC and not continuous.

4.4 CAPACITOR

Table 4.4.1 Capacitor trade and selection

Capacitor type	Total Capacitance	Total Voltage	Type of Arc
Disc Ceramic	0.04 µF	12000 V	Instantaneous
Silver Mica	0.00011 µF	10000 V	Instantaneous
Polypropylene	0.5 µF	9600 V	Sparked gaps

4.4.1 DISC CERAMIC CAPACITOR

The ceramic disc capacitors are manufactured by coating a ceramic disc with silver contacts on both sides and to achieve with the larger capacitance, these devices are made from multiple layers.

Figure 4.4.1.1 displays a capacitor bank with 0.04 μF capacitance and 12 kv capacity. Upon supplying high voltage, the capacitors gave a continuous output due to less capacitance. The charging and discharging rate is quite high for this capacitor bank.

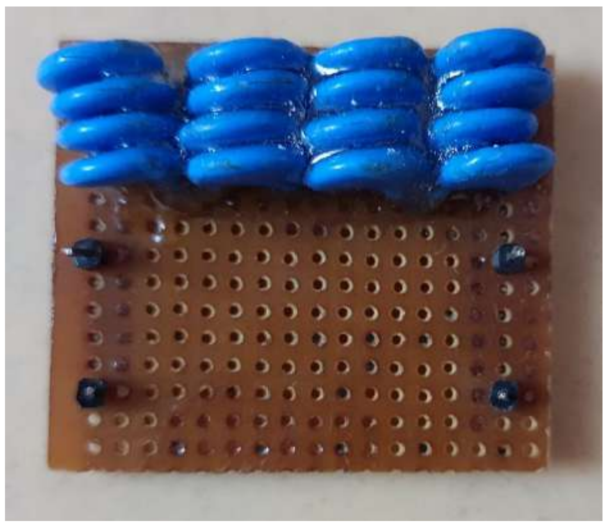

Figure 4.4.1.1 *Disc Ceramic Capacitors*

4.4.2 SILVER MICA CAPACITOR

The silver mica capacitors are prepared by sandwiching mica sheet coated with metal on both sides and this assembly is then encased in epoxy to protect the environment.

Figure 4.4.2.1 displays a capacitor bank with 0.00011 μF capacitance and 10 kv capacity. Upon supplying high voltage, the capacitors gave a continuous output due to very less capacitance. The charging and discharging rate is very high for this capacitor bank.

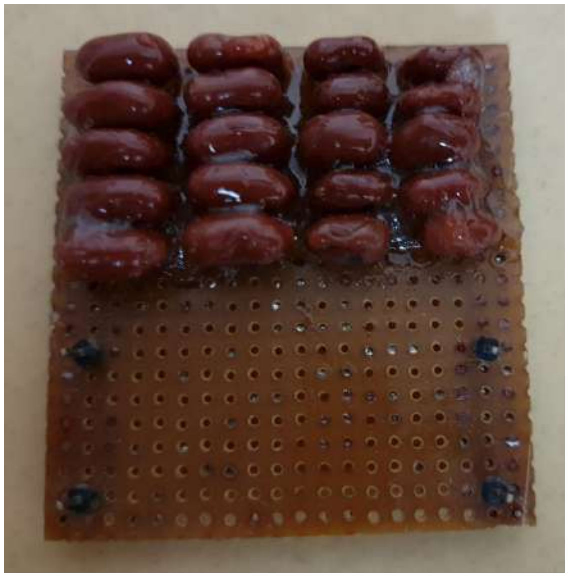

Figure 4.4.2.1 *Silver Mica Capacitors*

4.4.3 POLYPROPYLENE CAPACITOR

Film capacitors are made out of two pieces of plastic film covered with metallic electrodes, wound into a cylindrical shaped winding, with terminals attached, and then encapsulated.

Figure 4.4.3.1 displays a capacitor bank with 0.5 μF capacitance and 9.6 kv capacity. Upon supplying high voltage, the capacitors took time to get charged and gave a pulse of discharge as soon as the charge is built up enough for a discharge and the gap between both the output pins are nominal. The charging and discharging rate is much better for this capacitor. Due to the above reasons, Type J – Dipped Tantalum Capacitors is chosen as the capacitor for the capacitor bank of the thruster.

Figure 4.4.3.1 *Polypropylene Capacitors*

4.5 FLYBACK DRIVERS

Different drivers can be used for various power necessities and performances. Given below are the tradeoffs between few options explored.

4.5.1 MOSFET

Mosfets are similar to hard state relays and can be used for switching signals very efficiently. Figure 4.5.1.1 shows the schematic of the circuit. Low voltage DC is connected to the input of the circuit and primary of the transformer is connected to the other end. The module converts low voltage DC to high frequency pulsed DC and runs the flyback driver. Unfortunately, the mosfet is not strong enough to produce high voltage as well as the other drivers used. It produces a small spark for a little while before it blows up the mosfet attached to it. To prevent this, heat sinks can be added and more powerful mosfets can be used.

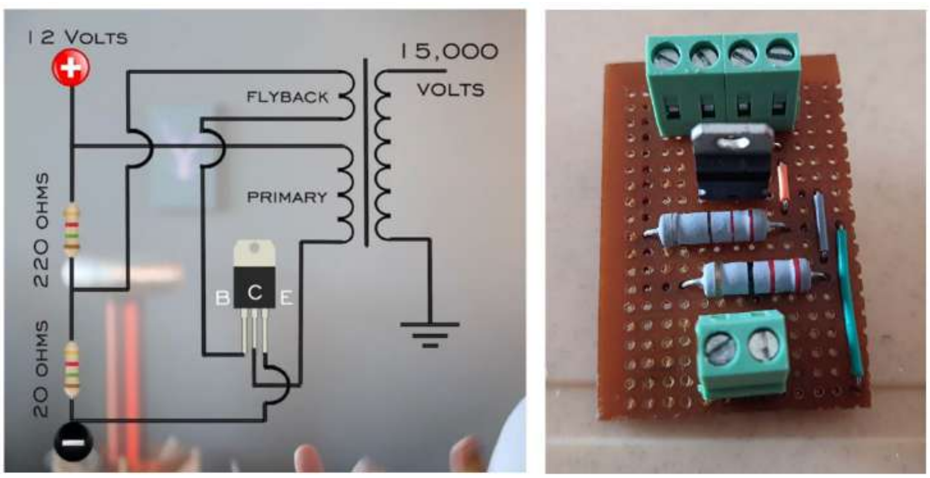

Figure 4.5.1.1 *Mosfet circuit [https://youtu.be/qaGmNRZG-Yg]*

4.5.2 555 TIMER

The 555 timer IC is a very cheap, popular and useful precision timing device which can act as either a simple timer to generate single pulses or long time delays, or as a relaxation oscillator producing a string of stabilized waveforms of varying duty cycles from 50 to 100%.

The 555 timer chip is extremely robust and stable 8-pin device that can be operated either as a very accurate Monostable, Bistable or Astable Multivibrator to produce a variety of applications such as one-shot or delay timers, pulse generation, LED and lamp flashers, alarms and tone generation, logic clocks, frequency division, power supplies and converters etc.

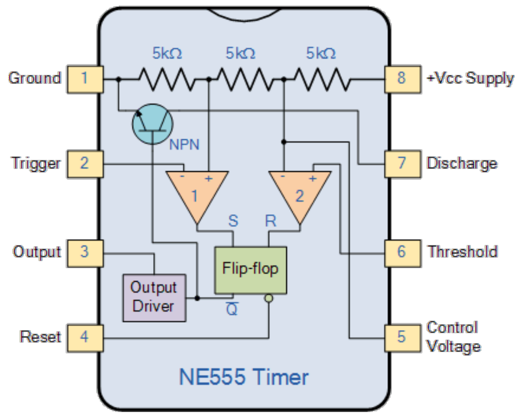

Figure 4.5.2.1 *555 timer circuit*

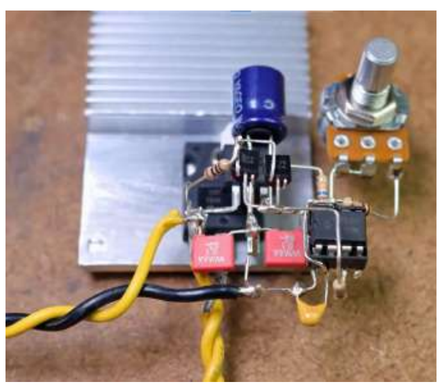

Figure 4.5.2.2 *555 timer circuit for driving flyback transformer [https://youtu.be/LhVx6I140Bk]*

4.5.3 ZVS INDUCTION HEATER CIRCUIT

Onboard the cubesat, DC supply is required to power the thruster. ZVS induction module gives us an option to supply the module with 12V DC at 2 amps to fire up the flyback transformer. Teflon easily ablated when the output from flyback was used to ignite it.

The ZVS circuit outputs high frequency pulsed DC. This is supplied to the primary coils of the transformer. Basically current flows front and back through the primary coil at high frequency thereby creating high voltage arc at the end points of the transformer.

Figure 4.5.3.1 *ZVS Induction Heater*

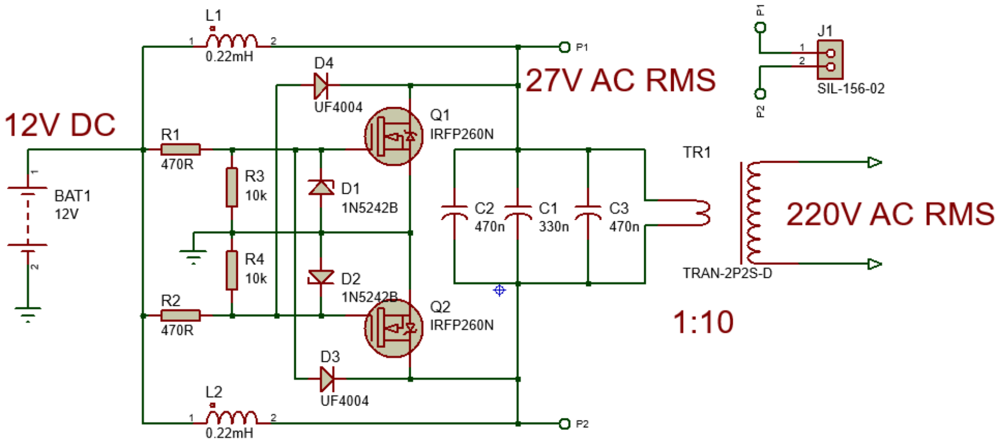

Figure 4.5.3.2 *ZVS Induction Heater Schematic*

4.5.4 ELECTRICAL BALLAST

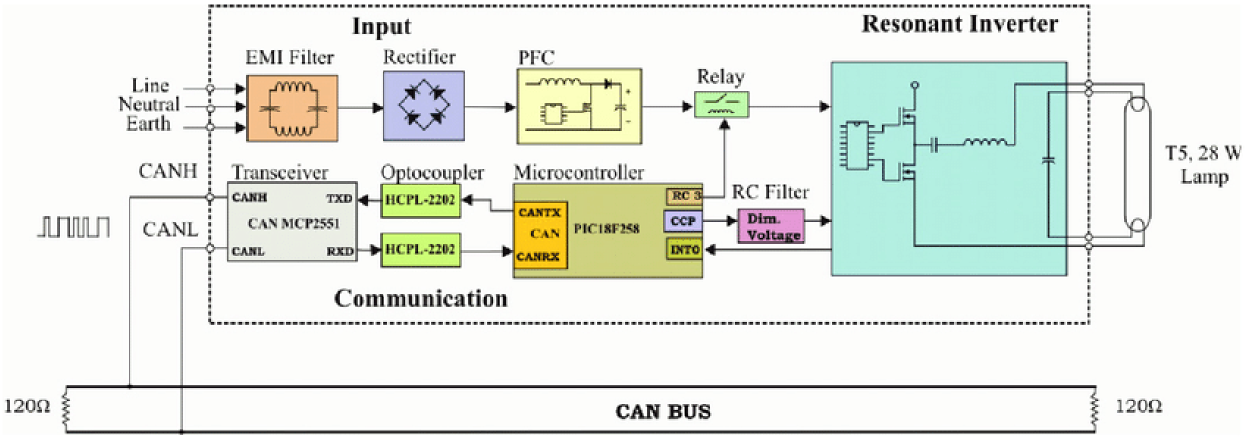

Figure 4.5.4.1 *Electrical Ballast Schematic [13]*

These are conventional chokes found in old day tubelights. They are supplied with 230V AC at 50Hz frequency and they give out high frequency AC in the range of 20KHz. This high frequency can be supplied to the primary pins of the flyback transformer. Out of the four pins that come outside from the ballast, only two pins give out AC voltage which are found using a multimeter. Different ballasts gave different outputs from the flyback transformer. Due to its simplicity and better efficient output, this was selected as our flyback driver.

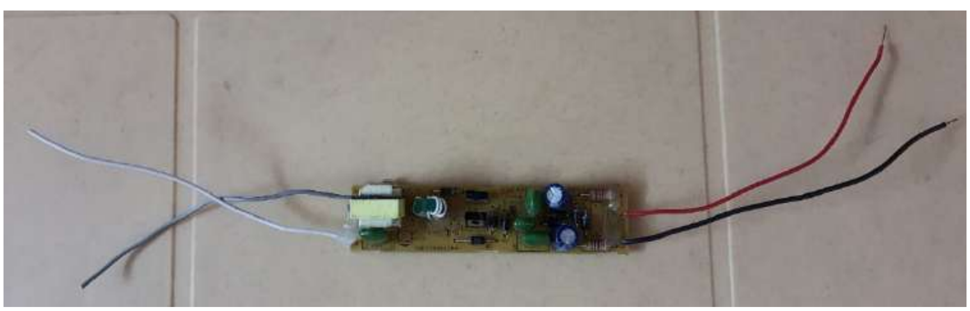

Figure 4.5.4.2 *Electrical Ballast used*

CHAPTER 5
HIGH VOLTAGE MEASUREMENT SYSTEM

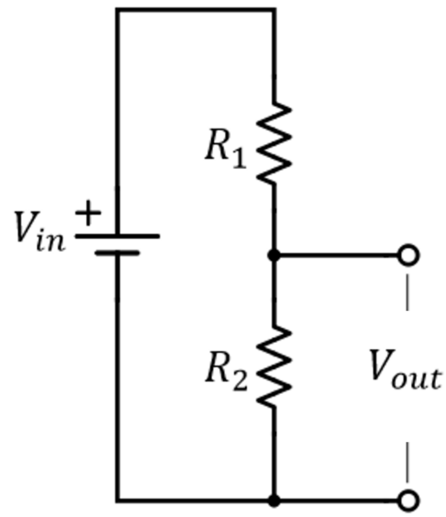

Figure 5.1 *Voltage divider*

Conventional multimeters have options to measure voltages ranging from 0-600v only. So to measure high voltages above the given range, Voltage dividers are used. Figure 5.1 shows the schematic of the voltage divider where V_{in} is the supply voltage and V_{out} is the output voltage. Two resistors R_1 and R_2 values are set for optimal output ranges. Using the formula given below, any of the four variables can be found out if three of the variables are known.

$$V_{out} = \frac{V_{in}R_2}{R_1+R_2} \qquad (5.1)$$

Flyback transformers are known for giving output in the range of 10- 25kv.

Let Input voltage = 25kv

$R_1 = 5x10^9\ \Omega$

$R_2 = 5x10^4\ \Omega$

Then output voltage will come around to be 25 volts which can be measured using a normal multimeter.

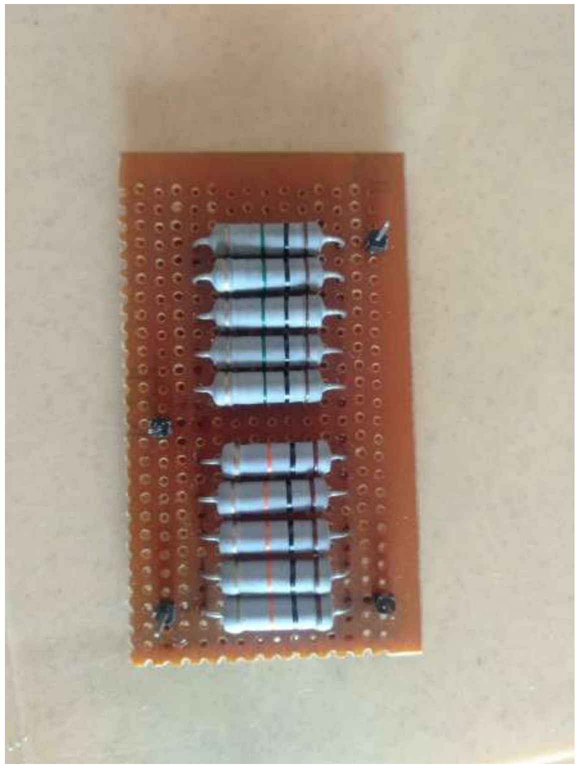

***Fig 5.2** Custom designed high voltage-voltage divider*

Using the above module, we can deduce the input voltage based on the output received from the transformer.

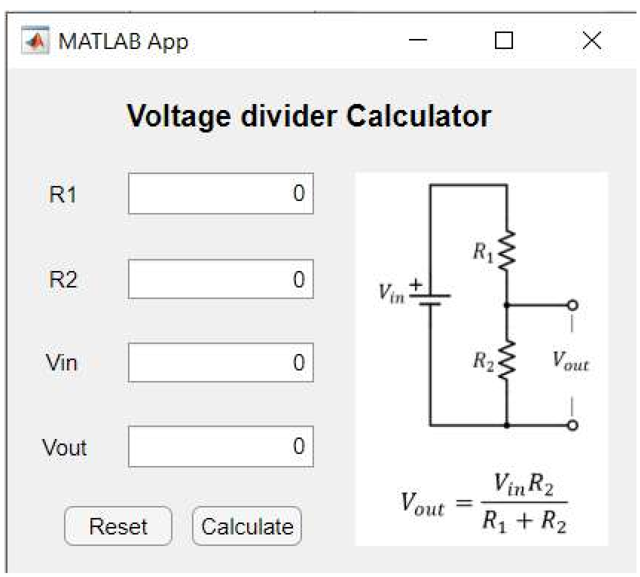

***Fig 5.3** Matlab app designed for measuring input voltage*

To ease the process of finding the input voltage, a Matlab app was designed as shown in Figure 5.4

CHAPTER 6

THRUST MEASUREMENT SYSTEM

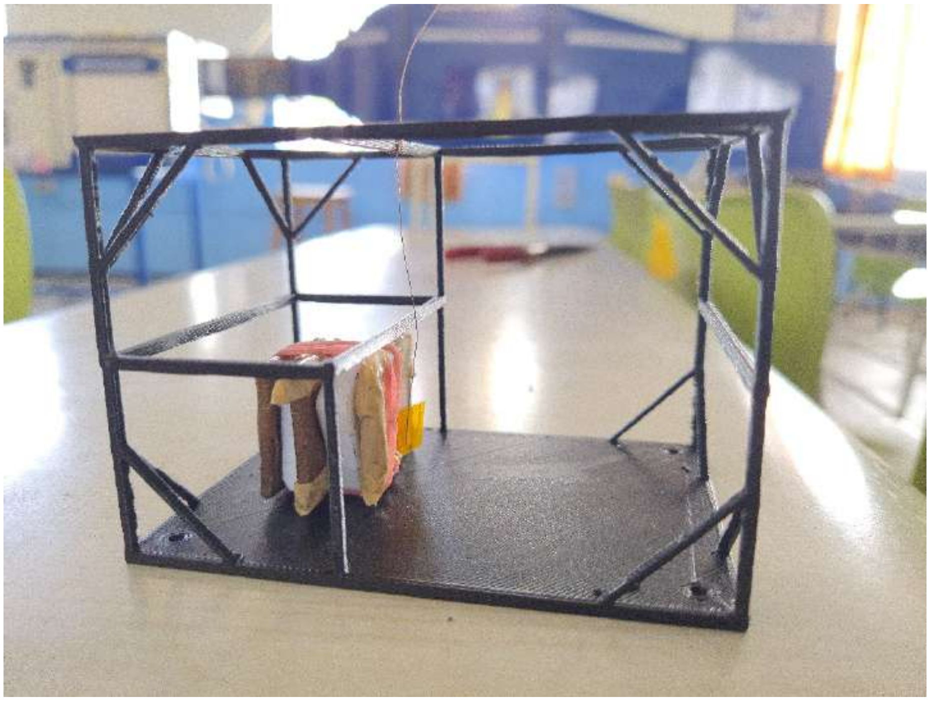

Fig 6.1 Custom made thrust measurement system

To measure the thruster produced from the thruster, the model in Figure 6.1 was used. The model is designed in Autodesk fusion 360 and 3d printed in PLA material.

The pendulum is made up of two pieces of 1x1 cm kapton tape and a copper rod of 40 AWG that extends from the top to the center of the kapton tape. The length of the wire is fixed such that the flapper is aligned to the centre of the output anode from the thruster. The length of the wire is 6.5cm.

Using the formula given below, Impulse bit of the thruster can be found. This is a formula formulated by Aheieva *et al* (2015) for calculating thrust of their Vacuum arc thruster. [6]

$$I_{bit} = m\sqrt{2 * g * (L - \sqrt{L^2 - x^2})} \text{……………….(6.1)}$$

Where

$I_{bit} = Impulse\ Bit\ (Ns)$

$m = mass\ of\ pendulum\ (kg)$

$g = acceleration\ due\ to\ gravity\ (m/s2\ )$

$L = length\ of\ pendulum\ (m)$x

$x = displacement\ of\ pendulum\ (m)$

We can get total impulse by multiplying impulse bit with the total number of firing of the thruster.

For calculating force, the following formula can be used.

$$F = \frac{m\sqrt{2*g*(L-\sqrt{L^2-x^2})}}{\Delta t} \text{……………………….(6.2)}$$

Where

F=Force

Δt =*discharge time*

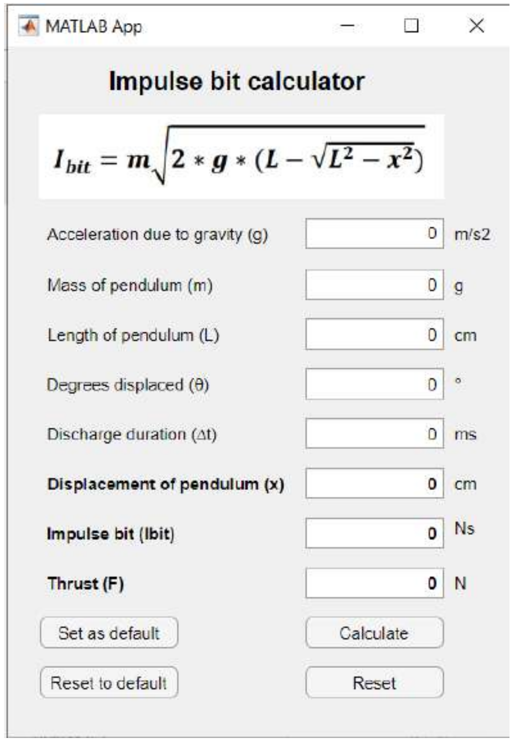

Fig 6.2 *Thrust measurement app*

To ease the process of finding thrust, a Matlab app was designed which inputs parameters like acceleration due to gravity, mass of pendulum, length of pendulum, degrees displaced and discharge duration and gives impulse bit and thrust as output.

CHAPTER 7

VACUUM CHAMBER SETUP

Pulsed plasma thrusters are operated in orbit where the satellite experiences microgravity. To simulate the effects of vacuum on the thruster, vacuum chamber was designed. The following are the different iterations of vacuum chamber till an optimal design is found.

7.1 GLASS JAR CHAMBER

Components used-

- Vacuum pump or syringe
- One side valves
- Glass jar

Dimensions-

- Height - 150mm
- Diameter - 100mm
- Volume- 1.1781×10^6 mm^3

Pump specifications-

- Input voltage – 12V DC
- Input current – 1.2A
- Capacity – 480 litres/hour

Figure 7.1.1 *Glass jar chamber Component*

Vacuum pump or a hand pump can be used to remove air from the jar container. The one stop valve makes sure that air doesn't get inside the jar once removed. In Figure 7.1.2, we can see a slightly inflated balloon placed inside the jar. Once the pump is turned on, air is pumped out and the balloon seems to inflate as shown in Figure 7.1.3. This is due to the pressure difference inside the balloon and the space between outside the balloon and inside the walls of the jar. The test was a success but the test section was too small to equip all the components of the current thruster.

Figure 7.1.2 *Glass jar chamber test - before*

Figure 7.1.3 *Glass jar chamber test - after*

7.2 GLASS TANK CHAMBER

Components used-

- Glass plates
- Silicone
- T- joint ¼ inch
- Ball valves ¼ inch
- Male couplers ¼ inch
- Female couplers ¼ inch
- ¼ inch collar
- Teflon tape
- Dendrite adhesive
- Vacuum pressure gauge
- Glass putty
- Clay

Dimensions-

- Height – 250 mm
- Length – 300 mm
- Width – 200 mm
- Volume – 1.5 x 10^7 mm^3

Pump specifications-

- Name – Polyvac vacuum pump
- Motor voltage – 230V/50HZ
- Motor Power – 750W
- Pump speed – 2800 rpm
- Vacuum speed – $20m^3/h$
- Rated pressure – 200PA

***Figure 7.2.1** Glass tank parts used*

Once all the components are collected, the assembly process began. Four plates are glued together in the orientation shown in Figure 7.2.2 using silicone sealant.

The chamber is then left for drying out the silicone. Paper tape is used to give additional support and stiffness for the chamber to hold together as shown in Figure 7.2.2.

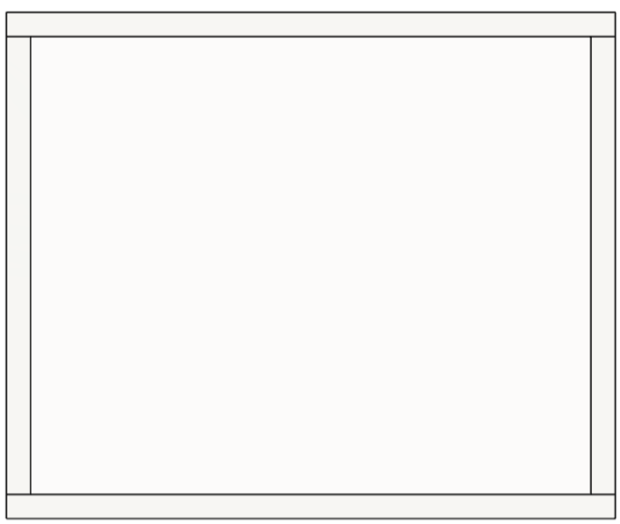

Figure 7.2.2 Glass tank v1 body assembly top view

Figure 7.2.3 shows the way rubber sheets will be placed on the top lid of the vacuum chamber facing downwards as a support for filling the gap with RTV silicone for gasket. For supplying power inside the vacuum chamber, a feedthrough vacuum chamber is designed with 4 copper rods inserted inside the top of the vacuum chamber. Two female couplers are also inserted into the led for connecting valve and Vacuum gauge for controlling the intake and outtake of air.

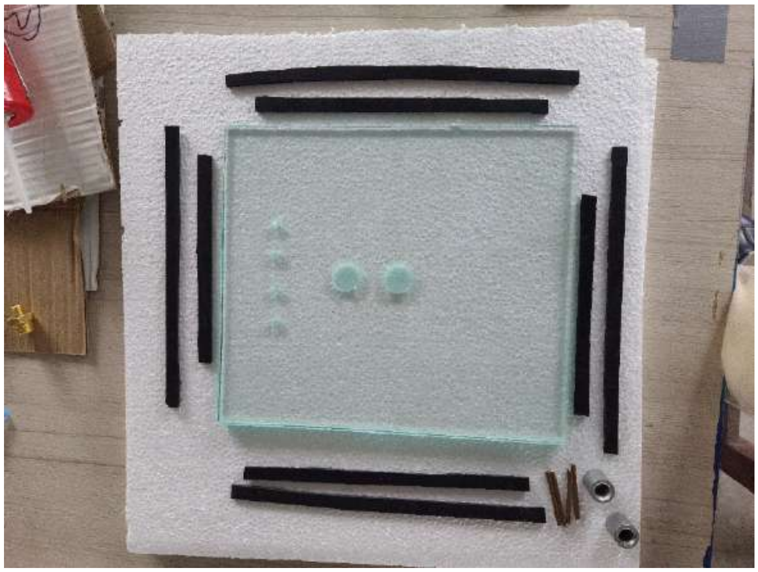

Figure 7.2.3 *Glass tank top part assembly*

Figure 7.2.4 *Glass tank body assembled*

After RTV silicone is filled up, the body of the vacuum chamber is placed on top of the gap to create an impression for the gasket.

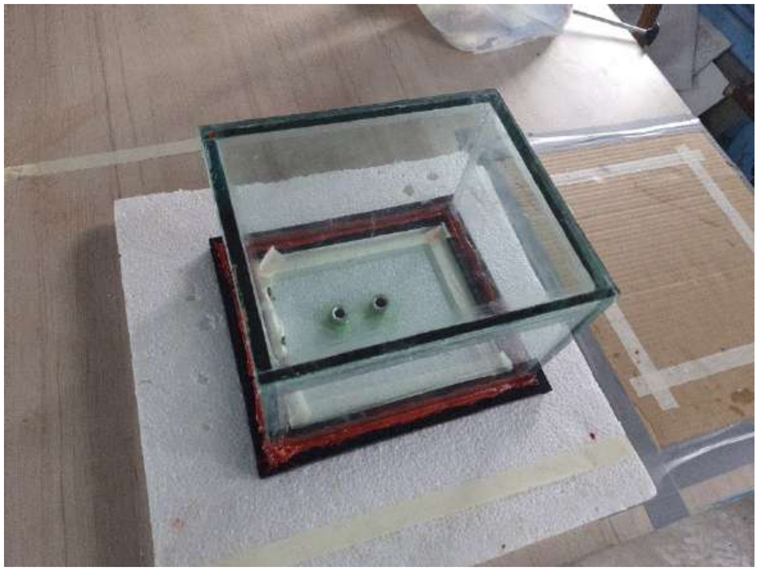

Figure 7.2.5 *RTV silicone applied*

After letting the RTV silicone dry, we realized that the weight of the tank was too much that the edges of the chamber almost touched the led through the silicone. It became impossible to open the led with an intact RTV gasket.

Figure 7.2.6 *Glass tank v1*

After managing to rip apart the led from the body, the led was cleaned off and one layer of rubber sheet was placed on the led right above the rims of the vacuum chamber. Then heat foam sheets were cut and placed under the lid. This provided quite some insulation and we were able to suck some amount of air out until the chamber imploded as shown in Figure 7.2.8. This was due to the orientation of the glass walls placed.

Figure 7.2.7 *Glass tank v2*

Figure 7.2.8 *Glass tank v2 implosion*

Another vacuum chamber with a different orientation of glass walls as shown in Figure 7.2.9 was then again fabricated.

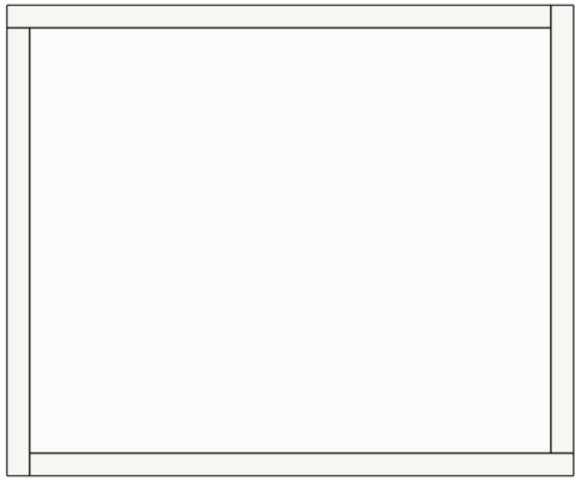

Figure 7.2.9 *Glass tank v3 body assembly top view*

Glass putty was used as a sealant this time due to its rigid properties. But opening the chamber again became a hassle because the glass putty never dried properly. But it was able to seal the chamber properly unlike the heat foam used earlier.

Figure 7.2.10 *Glass tank v3*

Finally, we settled with clay because it was quite hard and rubbery and easy to remove and apply compared to the other alternatives. But using this chamber, we reached only about 50% vacuum to make sure it doesn’t fail again.

Figure 7.2.11 *Glass tank v4*

7.3 ACRYLIC TUBE CHAMBER

Components used-

- 5 mm thick acrylic tubes
- 25 mm thick acrylic plate
- Wood Screws
- Silicone
- T- joint ¼ inch
- Ball valves ¼ inch
- Male couplers ¼ inch
- Female couplers ¼ inch
- ¼ inch collar
- Vacuum pressure gauge
- Mild steel plate
- Rubber gasket
- Clay

Dimensions-

- Height of test section – 400 mm
- Outer diameter – 310 mm
- Wall thickness – 10 mm
- Volume – 3 x 10^7 mm^3

Pump specifications-

- Name – Polyvac vacuum pump
- Motor voltage – 230V/50HZ
- Motor Power – 750W
- Pump speed – 2800 rpm
- Vacuum speed – $20m^3/h$
- Rated pressure – 200PA

To improve the vacuum percentage, we decided to make another vacuum chamber which can get close to absolute vacuum.

Two 5mm thick acrylic tubes were placed inside each other and closed with another acrylic lid. This was placed inside a mild steel base which has an engraving of about 7 mm deep cut along the circumference of the acrylic tubes put together. A silicone rubber gasket was bought commercially and placed inside the cut for better sealing solution for the vacuum chamber.

Simulation was done using Autodesk Fusion 360. Negative pressure of 0.99 bar was applied to the inner walls of the vacuum chamber as shown in Figure 7.15.

With negative 0.99 bar, the chamber can theoretically sustain 97.4% vacuum at 0.03 atm.

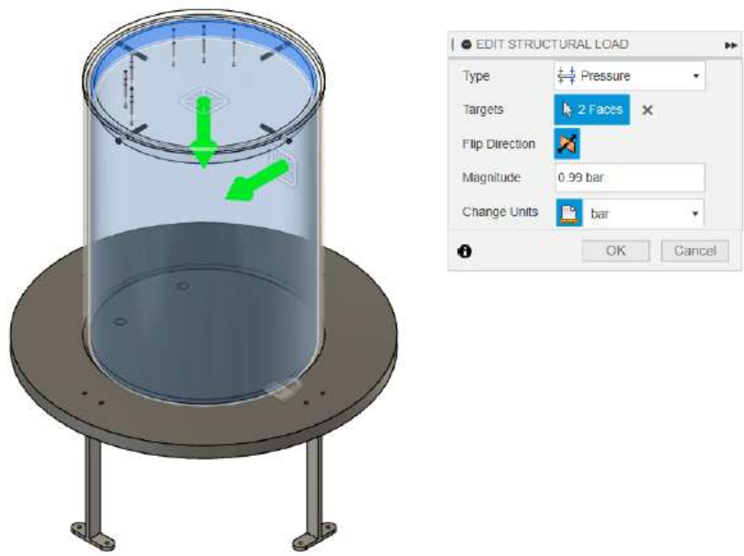

Figure 7.3.1 *Acrylic tube chamber simulation loads*

The simulation results were promising as shown in Figure 7.3.2. Maximum displacement was only 0.08576 mm and the safety factor was 15.

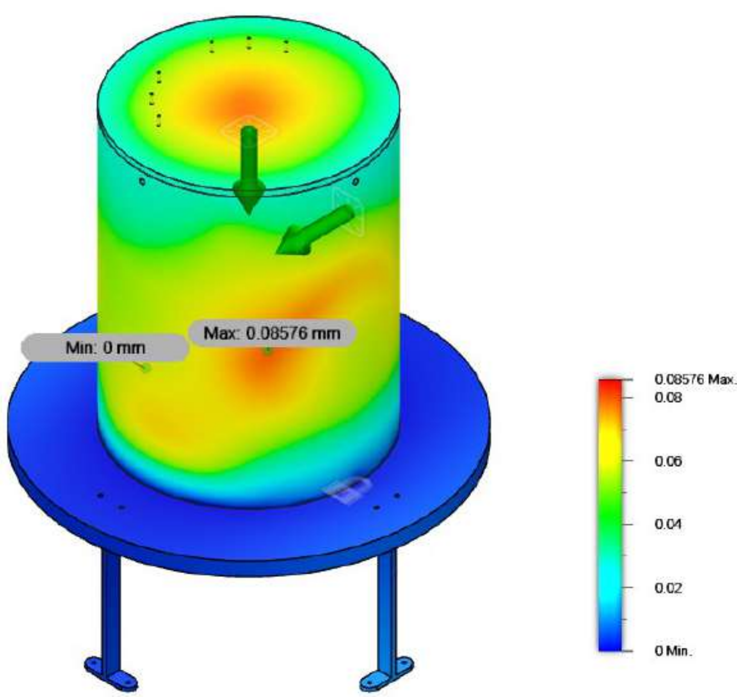

Figure 7.3.2 *Acrylic tube chamber simulation results*

The mild steel based was lathed and I sections were screwed to the base for support. The acrylic tubes and the lid is screwed together using wood screw and silicone sealant is also applied to the joints for a better seal. Clay is applied to the base of the chamber for sealing all leaks.

***Figure* 7.3.3** *Acrylic tube chamber setup*

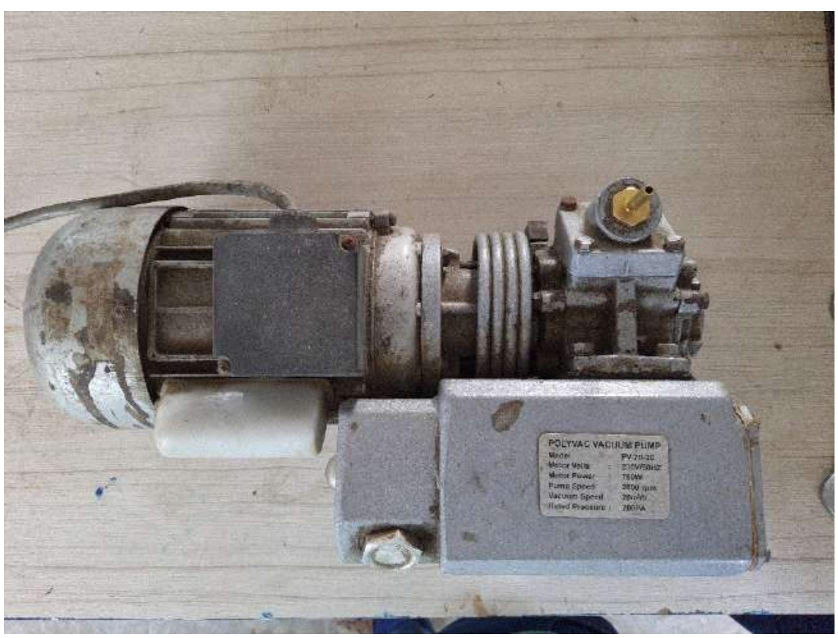

***Figure* 7.3.4** *Vacuum pump*

CHAPTER 8

EXPERIMENTAL SETUP

8.1 MECHANICAL SETUP

The environment in which the thruster is set to be tested in vacuum. Custom feedthrough vacuum chambers were designed for supplying power to the thruster through the chamber. Figure 8.1.1 depicts the overall experimental setup. A vacuum pump is first used to create vacuum inside the chamber. AC and DC voltage are supplied to the vacuum chamber through 6 copper rods. The vacuum chamber is an acrylic tube chamber with a mild steel base. A vacuum pump is used to remove air from the chamber. The vacuum chamber setup is explained in detail in Chapter 7.

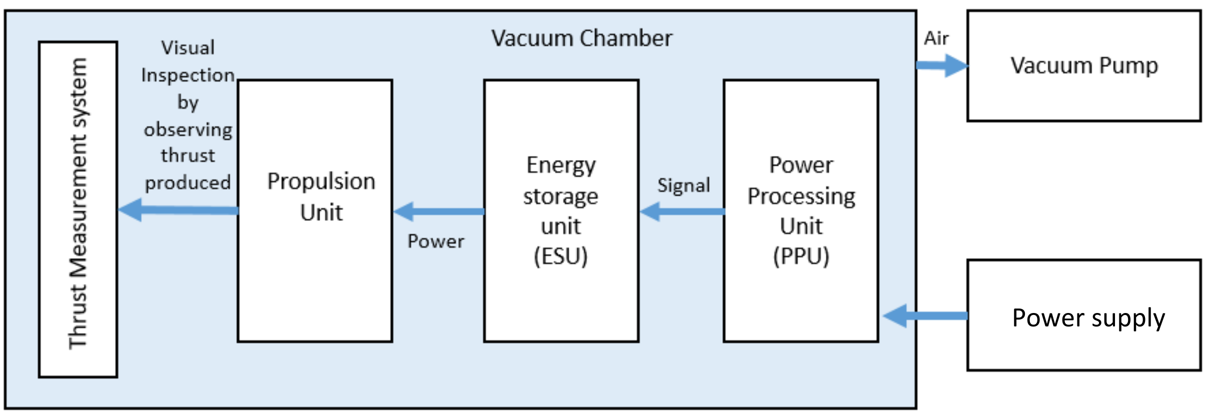

Figure 8.1.1 Experimental Setup Overview

8.2 ELECTRONIC SETUP

An Arduino promini is placed inside the chamber which is connected to a relay which switches AC signal between two electrical ballasts which in turn power two flyback transformers that charge two capacitor banks connected to the Thruster.

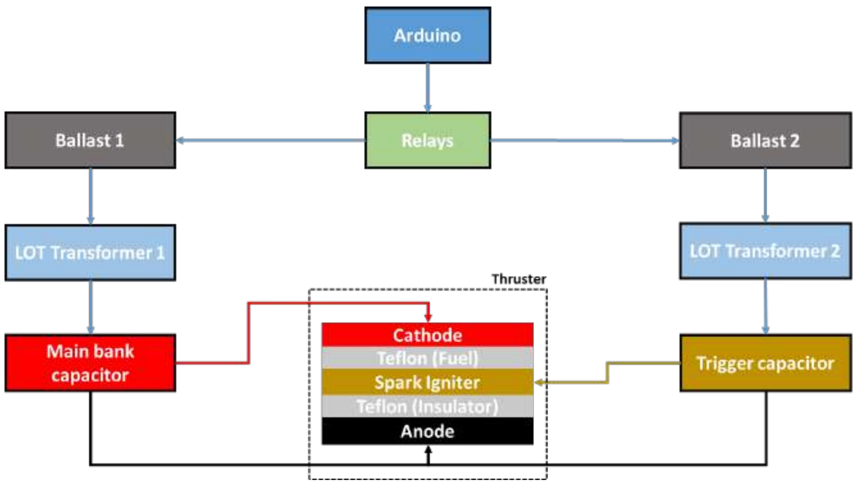

Figure 8.2.1 Signal Flowchart through components

Figure 8.2.1 shows the flow of signal through the circuit. DC 5v is supplied to Arduino externally to power it up. It is connected to a dual channel 5v relay for switching signal for charging and discharging capacitor banks. Signals switch between two electrical ballast connected to the relay. The ballasts are powered externally using AC supply 230V at 50Hz. They output high frequency AC supply in the order of 20KHz. This is supplied to the primary coil of the Flyback/Line output transformer (LOT). The transformer produces high voltage across the secondary coil in the range of 20kv. The output is rectified inside the transformer using multiple diodes so it gives out 20kv DC as output. Two capacitor banks are charged using this voltage for a main discharge and for triggering a spark for breakdown of voltage across the plates.

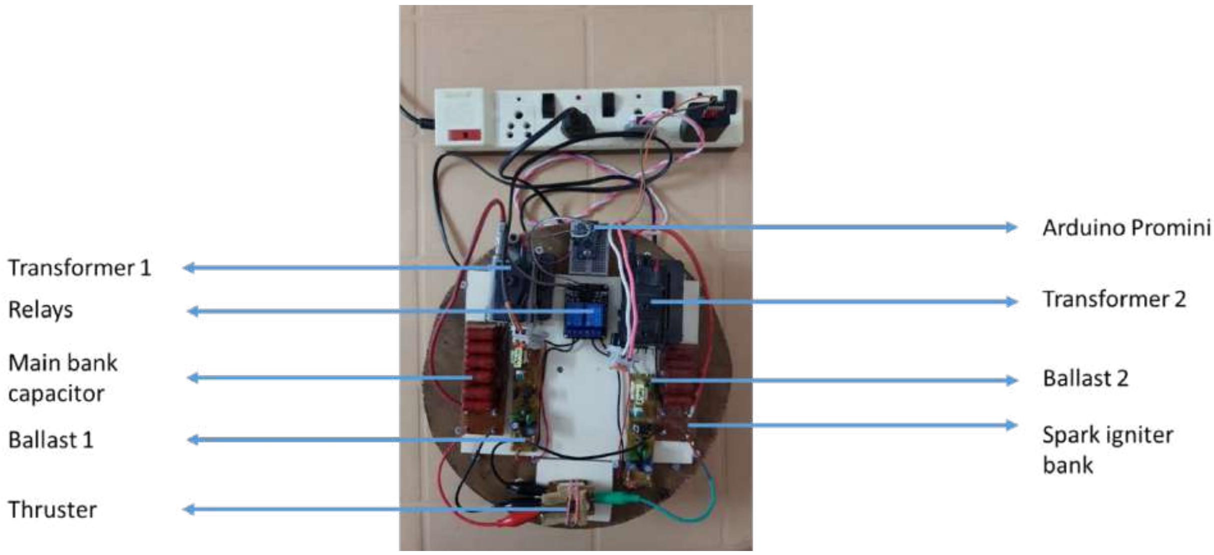

Fig 8.2.2 Components used

Figure 8.2.2 displays the components orientation setup on a wooden stand to prevent power transfer from the modules to the mild steel base. Plastic legs are used for electrical catastrophe prevention.

8.3 WORKING OF THE THRUSTER

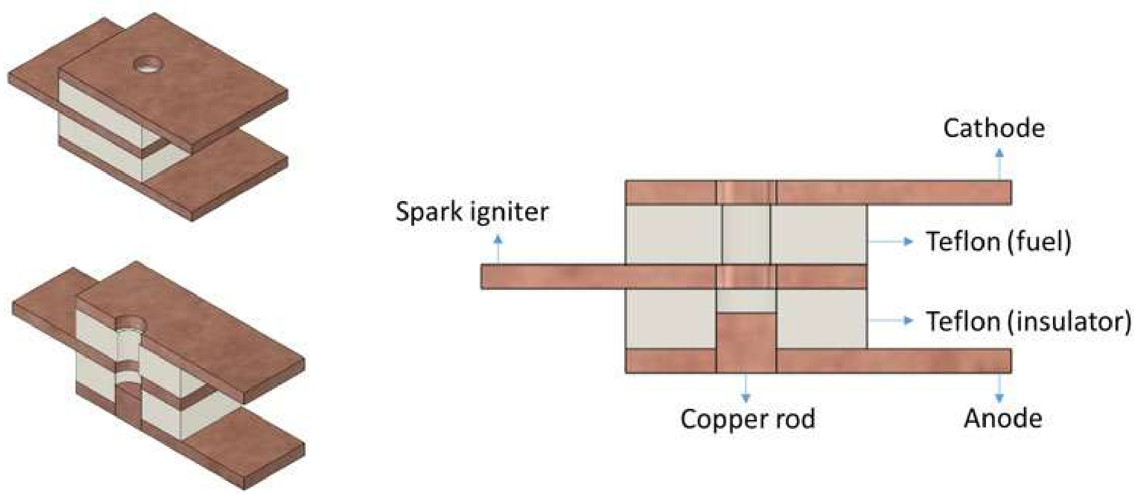

***Fig 8.3.1** Pulsed plasma thruster cross sectional view*

Fig 8.3.1 shows the orientation of components used in the pulsed plasma thruster. It consists of three copper plates – Anode, Cathode and Spark igniter. High voltage positive supply is supplied to the Cathode and negative supply to the anode. The positive supply of the trigger supply is supplied to the spark igniter rod and the negative to the same anode. A small copper rod is also inserted inside the anode for Teflon ablating purpose.

When high voltage is supplied to the end terminals through capacitor bank, the arc gap in between them prevent them from arcing. When a quick spark is introduced between the spark igniter plate and anode, the air gets ionized around the area and facilitates an arc between cathode and anode. When the arc forms, it ablates a little portion of the propellant and ionizes the propellant dust into propellant plasma which is expelled out through the opening on the top. This produces thrust and pushes the spacecraft forward.

8.4 COMPONENT FAILURES

8.4.1 CAPACITOR FAILURE

Fig.8.4.1.1 *Damaged capacitor bank*

Capacitor banks of different types of capacitors were tested and out of them propylene capacitors were selected because of the long discharge time they possess. Due to this property, if we charge up the capacitor upto a point where it cant take up any more power and the gap between the terminals are greater than nominal values, it tends to explode and cause a short circuit.

8.4.2 RELAY FAILURE

If the AC power supplies connected to the relay module are turned on even in Normally closed (NC) state, the circuit shorts and causes the relay to fail. But it doesn’t stop there and goes on to damage the Arduino connected to the relay too.

8.4.3 BALLAST FAILURE

Different brands of ballast gave different output and thereby varied voltage output from transformers as well. As of now, Crompton tube light ballasts are used as they proved to be stable for a lot of tests even though their performance reduced at one point. Replacing the ballast fixed the issue. Phillips ballast provided much greater output compared to Crompton ballasts, but failed to function properly even after 10 tests.

CHAPTER 9

EXPERIMENTATION AND RESULTS

9. 1 EXPERIMENTAL PROCEDURE

1. All the components are connected based on the schematics.
2. Arduino is initially powered up before the AC supplies are turned on. This is to check if arduino is powered properly and to ensure that the relay doesn't fail if it isn't.
3. Then the power is turned off and ac supplies are connected to the junction box.
4. The whole setup is turned on and working of thruster is verified.
5. The holes in the thruster's centre are aligned properly.
6. The top lid of the chamber is placed on top of the mild steel base.
7. Vacuum pump is turned on and the vacuum gauge is monitored to check the pressure difference.
8. Once the vacuum gauge reads -28 inch Hg, the vacuum pump is turned off.
9. Step 2 is performed again to ensure there are no faulty connections
10. The whole setup is then turned on.
11. The thruster produces thrust which is measured using a thrust measurement system.
12. Operation of the thruster is recorded (in such a way that the angle formed by the measurement system is visible in the video).
13. Different experiments are performed to check the characteristics of the thruster and videos are recorded.
14. Air is then let into the chamber by opening a ball valve.
15. The setup is then disassembled.

Fig 9.1.1 *Thruster setup inside the vacuum chamber*

Fig 9.1.2 *Vacuum gauge pressure reading*

(-28 inHg relates 94% vacuum at 0.06 atm)

9.2 FORMULA USED

$$I_{bit} = m\sqrt{2 * g * (L - \sqrt{L^2 - x^2})} \quad \text{...............(9.2.1)}$$

Where

I_{bit} = $Impulse\ Bit\ (Ns)$

m = $mass\ of\ pendulum\ (kg)$

g = $acceleration\ due\ to\ gravity\ (m/s2)$

L = $length\ of\ pendulum\ (m)$

x = $displacement\ of\ pendulum\ (m)$

Mass of pendulum = Mass of kapton tape+ mass of copper wire

= 0.0071g+ 0.00319g

= 0.01029g

- Dimension of kapton tape – 1x1x0.005mm
- Average density of kapton tape – 1.42 $\frac{g}{cm^3}$
- Copper wire – length 6.5 cm, Diameter 0.008 cm
- Average density of copper – 8.96 $\frac{g}{cm^3}$

For calculating force, the following formula can be used.

$$F = \frac{m\sqrt{2*g*(L-\sqrt{L^2-x^2})}}{\Delta t} \quad \text{.........................(9.2.2)}$$

Where

F=Force

Δt =*discharge time*

9.3 OBSERVATION

Table 9.3.1 Experiment observation

Vacuum %	Charging time	Angle displaced (θ)	Displacement (cm)	Impulse bit (Ns)
0		36°	4.084	5.321×10^{-6}
25		30°	3.403	4.345×10^{-6}
50	200ms	24°	2.723	3.425×10^{-6}
75		20°	2.269	2.832×10^{-6}
94		17°	1.929	2.396×10^{-6}

9.4 RESULTS

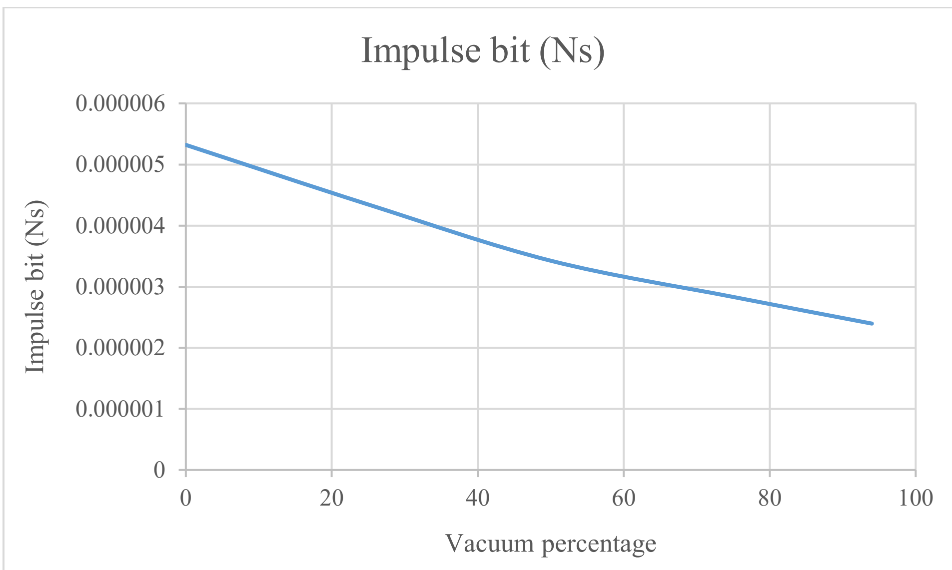

***Fig.9.4.1** Experiment result*

It is observed that the performance of thruster reduces in vacuum. Contrary to the prediction, it is probably due to the different characteristics of the capacitor in vacuum that is causing this drawback. Nevertheless, the impulse bit measured in absolute vacuum matches the impulse bit readings of other pulsed plasma thruster and is well within its general operating range.

CHAPTER 10
MODEL VALIDATION

Our model is based on a Pulsed plasma thruster designed by Michael Bretti, Founder of Applied Ion Systems LLC, a unique open-source electric propulsion R&D company in the aerospace field leading developments of ultra-low cost micro plasma and ion thrusters for nanosatellites.

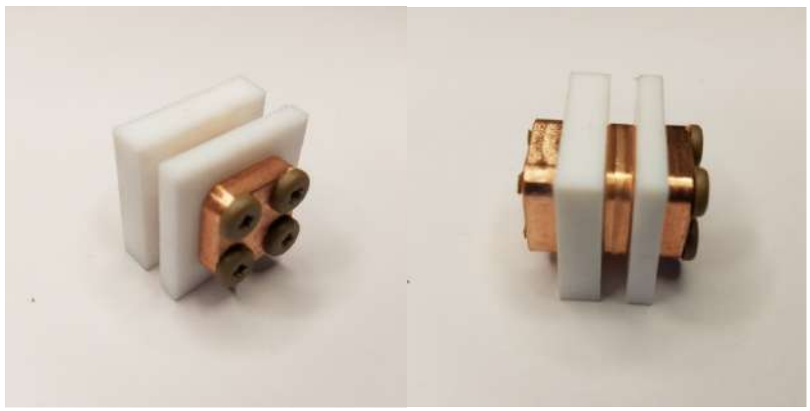

Fig. 10.1 *AIS-gPPT3-1C Single-Channel Gridded Pulsed Plasma Thruster*
Credits- Applied Ion systems

Stacked pulsed plasma thruster have a much simpler mechanism comparative to a conventional pulsed plasma thruster. A similar model based on AIS-gPPT3-1C was designed to test the working as shown in Figure 10.2.

Fig. 10.2 *Pulsed plasma thruster used*

AIS-gPPT3-1C was designed to incorporate the electronics part of the thruster miniaturized with the thruster. The whole experimental setup tested so far by our team is displayed in Figure 10.4.

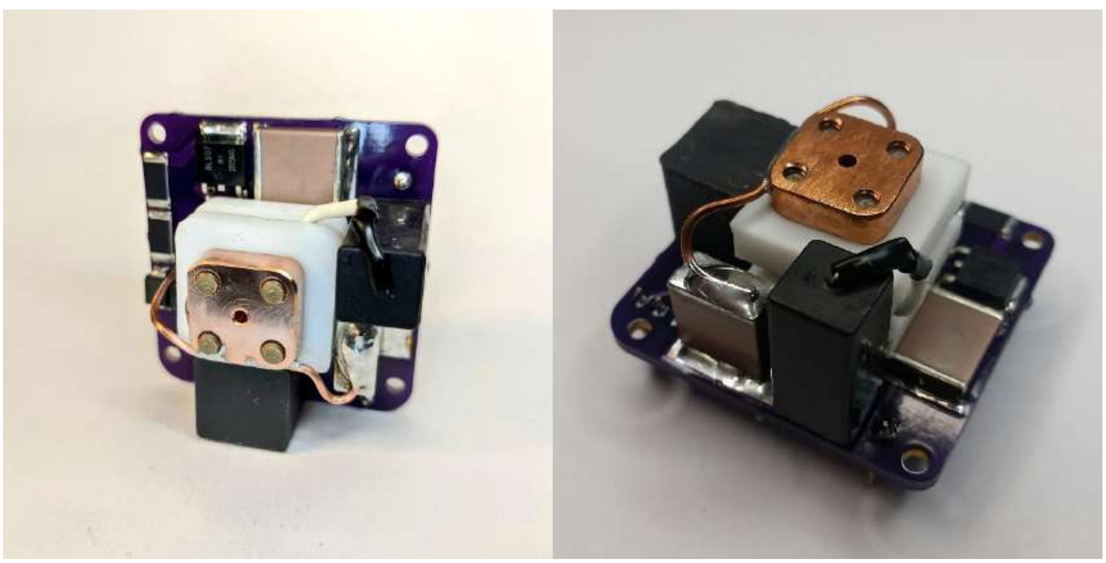

Fig. 10.3 *AIS-gPPT3-1C Series Integrated Propulsion Module*

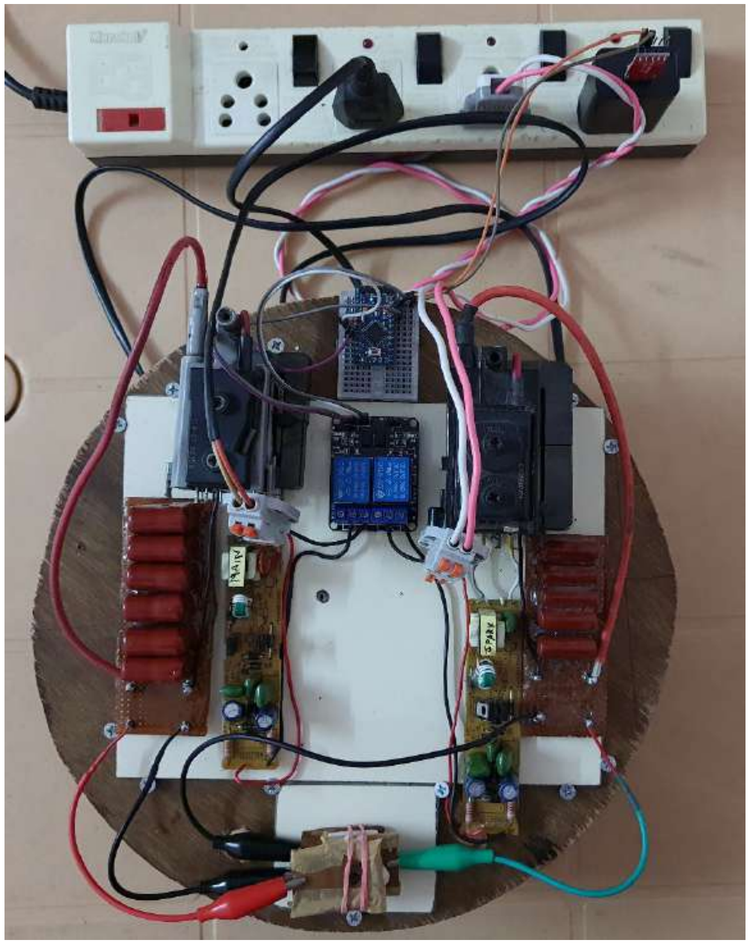

Fig. 10.4 *Thruster experimental setup*

Figure 10.5 shows the placement of electrodes and Teflon comparison between Michael Bretti's model and our model.

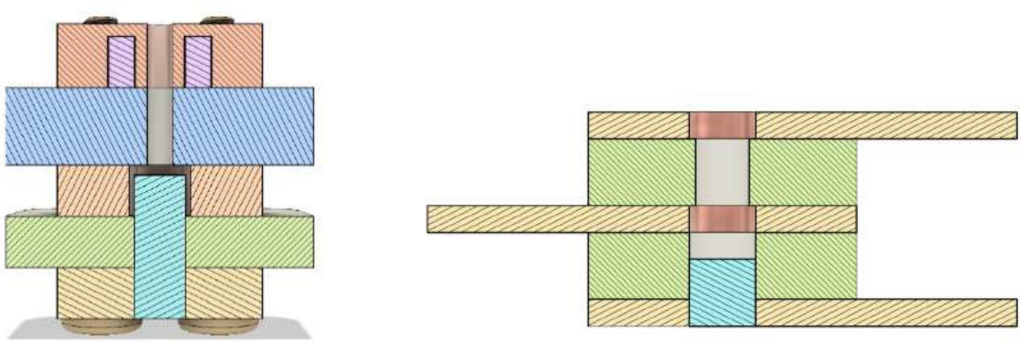

Fig. 10.5 *Stacked thruster orientation of AIS-gPPT3-1C (Right),*
Pulsed plasma thruster designed currently (Left)

Left photo in Figure 10.6 shows the thruster firing and the flapper getting ready to move. On the right we can see a similar photo captured by Michael Bretti of his thruster.

Fig. 10.6 *Capacitor discharging similarities*

For measuring impulse bit, angle displaced by the thruster is measured and a formula is used (explained in detail in Chapter 6). Figure 10.7 is a comparison of measuring angle between our and Michael Bretti's model.

Fig. 10.7 *Flapper forming angle due to the impulse provided by thruster*

RESULTS VALIDATION

Table 10. 1 Impulse bit measurements of AIS-gPPT2-1C

Credits- Applied Ion Systems

AIS-gPPT2-1C Impulse Bit Measurements - Test Data							
Shot #	**Time Stamp (s)**	**Charge Time (s)**	**Voltage (V)**	**Energy (J)**	**Angle (Degrees)**	**Displacement (cm)**	**I-Bit (uN-s)**
1	2	10	1300	0.84	35	2.10	3.52
2	11	9	1300	0.84	25	1.52	2.48
3	16	5	1296	0.84	18	1.10	1.77
4	20	4	1287	0.83	14	0.85	1.36
5	25	5	1296	0.84	14	0.85	1.36
6	29	4	1287	0.83	19	1.16	1.87
7	33	4	1287	0.83	26	1.57	2.57
8	34	1	890	0.40	14	0.85	1.36
9	36	2	1171	0.69	20	1.22	1.97
10	37	1	890	0.40	15	0.91	1.46
11	39	2	1171	0.69	22	1.34	2.17
12	41	2	1171	0.69	18	1.10	1.77
13	42	1	890	0.40	13	0.79	1.26
14	44	2	1171	0.69	13	0.79	1.26
15	45	1	890	0.40	8	0.49	0.78
16	46	1	890	0.40	8	0.49	0.78
17	47	1	890	0.40	11	0.67	1.07
18	48	1	890	0.40	12	0.73	1.17
19	50	2	1171	0.69	14	0.85	1.36
20	51	1	890	0.40	14	0.85	1.36
21	53	2	1171	0.69	13	0.79	1.26
22	54	1	890	0.40	16	0.97	1.56

Under 94% vacuum, the thruster produces around 2.5µNs to 4µNs as discussed in Chapter 9 similar to the readings by Michael Bretti.

CHAPTER 12

APPLICATIONS OF PULSED PLASMA THRUSTER

- The PPT typically flies in spacecraft using surplus power from abundant solar energy. PPT using solid propellant offers the benefits of the mission due to the simplicity of the system and the high specific impulse therefore suitable for tasks such as attitude control, station-keeping, orbital release operations, and space exploration on relatively small spacecraft weighing less than 100 kg.

- With the PPT, you can double the life of these small satellite missions without significantly increasing complexity or cost due to the inherent simplicity and relatively low cost of PPT. Because pulsed plasma thrusters are relatively simple and low cost associated with PPT compared to other forms of electric propulsion such as Hall-effect ion thrusters.

- For keeping the sun-synchronous orbit for a small satellite with the mass of 100 kg during 5 years a PPT is required, that is by 16 kg less than in the case of using propulsion system with hydrazine .

- Effective PPT application may be expected in the tasks of prolonging the period of active life for the small satellites by compensating the aerodynamic drag and increasing the height of their operation using the pulsed plasma thrusters.

- In the tasks of attitude control for the small satellites being the parts of navigation system, the attitude and orbit control system mass is reduced for as many as 15kg when its standard hand-wheel actuator devices are replaced by PPT therefore extending the mission duration of spacecrafts.

CONCLUSION

This paper discusses the whole process of fabricating a low cost pulsed plasma thruster model. A pulsed plasma thruster model is successfully designed and tested out. Trade and selection of various components were done to understand their characteristics and properties which influence the output from the thruster. Various measurement systems were also fabricated for testing respective parameters. The model is also validated based on prior work with promising results. Troubleshooting and finalizing the model took quite some time but it was worth the trouble went through.

FUTURE WORKS

- Optimizing the circuit by electrically sealing the circuit for any leakages.
- Testing the setup in absolute vacuum.
- Taking reading for different parameters of the thruster.
- Measure lifetime of the thruster.
- Miniaturizing the circuit such that it can be used as a propulsion unit in a 1U cubesat.
- Create a novel design for increasing efficiency of the pulsed plasma thruster

Appendix A

Arduino code

A.1 Capacitor charging

```
int Mainbank = 4;
int sparkigniter = 3;

void setup()
{
  pinMode(Mainbank, OUTPUT);
  pinMode(sparkigniter, OUTPUT);
}

void loop()
{
  digitalWrite(Mainbank, HIGH);
  delay(200);
  digitalWrite(Mainbank, LOW);
  digitalWrite(sparkigniter, HIGH);
  delay(100);
  digitalWrite(sparkigniter, LOW);
  delay(1000);
}
```

A.2 Voltage measurement

```
const int voltageSensor = A0;

float vout = 0.0;
float vin = 0.0;
float R1 = 30000.0;
float R2 = 7500.0;
int value = 0;

void setup()
{
Serial.begin(9600);
delay(2000);
}

void loop()
{
  value = analogRead(voltageSensor);
  vout = (value * 5.0) / 1024.0;
  vin = vout / (R2/(R1+R2));
  Serial.print("Input = ");
  Serial.println(vIN);
  delay(500);
}
```

Appendix B

Matlab codes

B.1 Voltage divider calculator

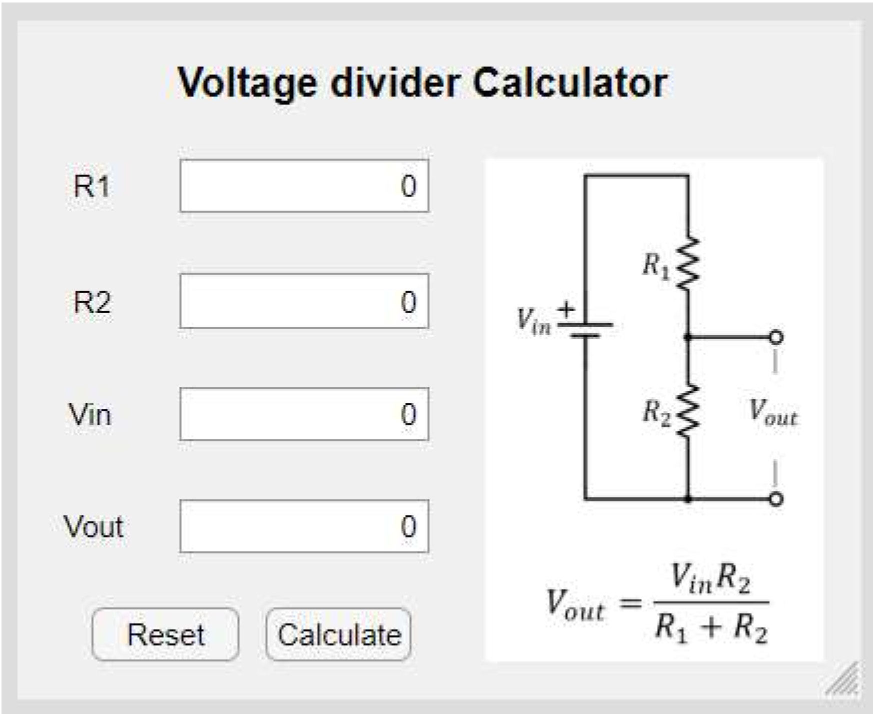


```
% Button pushed function: CalculateButton
    function CalculateButtonPushed(app, event)
        R1= app.R1EditField.Value;
        R2= app.R2EditField.Value;
        Vin= app.VinEditField.Value;
        Vout= app.VoutEditField.Value;

        if Vout == 0
            Vout=(Vin*R2)/(R1+R2);
            app.VoutEditField.Value= Vout;
        end
```

```
        if Vin == 0
            Vin=(Vout*(R1+R2))/R2;

            app.VinEditField.Value= Vin;

        end


        if R1 == 0
            R1=(R2*(Vin-Vout))/Vout;

            app.R1EditField.Value= R1;

        end


        if R2 == 0
            R2=(R1*Vout)/(Vin-Vout);

            app.R2EditField.Value= R2;

        end

    end

% Button pushed function: ResetButton
    function ResetButtonPushed(app, event)

        app.R1EditField.Value=0;

        app.R2EditField.Value=0;

        app.VinEditField.Value=0;

        app.VoutEditField.Value=0;

    end
```

B.2 Impulse bit calculator

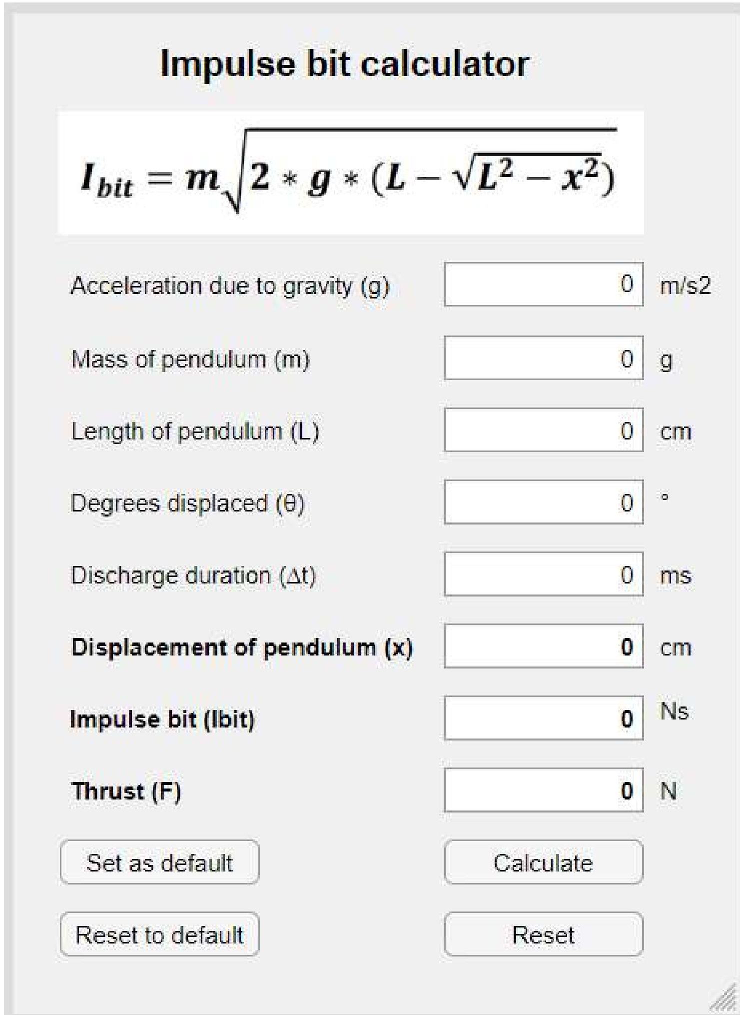


```
% Button pushed function: SetasdefaultButton
function SetasdefaultButton_2Pushed(app, event)
            app.g = app.AccelerationduetogravitygEditField.Value;
            app.m = app.MassofpendulummEditField.Value*0.001; %converting g to kg
            app.l = app.LengthofpendulumLEditField.Value*0.01; %converting cm to m
            app.theta = app.DegreesdisplacedEditField.Value;
        end


        % Button pushed function: ResettodefaultButton
        function ResettodefaultButtonPushed(app, event)
            app.AccelerationduetogravitygEditField.Value = app.g;
            app.MassofpendulummEditField.Value = app.m/0.001;
            app.LengthofpendulumLEditField.Value = app.l/0.01;
            app.DegreesdisplacedEditField.Value = app.theta;
            app.DegreesdisplacedEditField.Value = 0;
            app.DisplacementofpendulumxEditField.Value = 0;
```

```
    app.ImpulsebitIbitEditField.Value = 0;
    app.DischargedurationtEditField.Value = 0;
    app.ThrustFEditField.Value = 0;
end


% Button pushed function: ResetButton
function ResetButtonPushed(app, event)
    app.AccelerationduetogravitygEditField.Value = 0;
    app.MassofpendulummEditField.Value = 0;
    app.LengthofpendulumLEditField.Value = 0;
    app.DegreesdisplacedEditField.Value = 0;
    app.DisplacementofpendulumxEditField.Value = 0;
    app.ImpulsebitIbitEditField.Value = 0;
    app.DischargedurationtEditField.Value = 0;
    app.ThrustFEditField.Value = 0;
end


% Button pushed function: CalculateButton
function CalculateButton_2Pushed(app, event)
    app.g = app.AccelerationduetogravitygEditField.Value;
    app.m = app.MassofpendulummEditField.Value*0.001; %converting g to kg
    app.l = app.LengthofpendulumLEditField.Value*0.01; %converting cm to m
    app.theta = app.DegreesdisplacedEditField.Value;
    app.d = app.DischargedurationtEditField.Value*1000; %converting s to ms

    app.x = 2*pi*app.l*(app.theta/360);
    app.i = app.m*(sqrt(2*app.g*(app.l-sqrt(app.l.^2-app.x.^2))));

    app.DisplacementofpendulumxEditField.Value = app.x/0.01;%converting m to cm
    app.ImpulsebitIbitEditField.Value = app.i;

    if app.DischargedurationtEditField.Value ~= 0
        app.t = app.i/app.d;
        app.ThrustFEditField.Value = app.t;
    end
end
```

REFERENCES

[1] Burton, Rodney L., and P. J. Turchi. "Pulsed plasma thruster." *Journal of Propulsion and Power* 14.5 (1998): 716-735.

[2] Rezaeiha, Abdolrahim, and Tony Schönherr. "Overview of alternative propellants for use in PPT." *29th International Symposium on Space Technology and Science ISTS*. Vol. 2. No. 9. 2013.

[3] Nawaz, Anuscheh, et al. "Investigation of the magnetic field in a pulsed plasma thruster." *Aiaa Journal* 46.11 (2008): 2881-2889.

[4] Ciaralli, Simone. *A study of the lifetime of miniaturized ablative pulsed plasma thrusters*. Diss. University of Southampton, 2014.

[5] Aheieva, Kateryna, Kazuhiro Toyoda, and Mengu Cho. "Vacuum arc thruster development and testing for micro and nano satellites." *Transactions of the Japan Society for Aeronautical and Space Sciences, Aerospace Technology Japan* 14.ists30 (2016): Pb_91-Pb_97.

[6] Bingyin, Kang. "High voltage dc-dc converter for a pulsed plasma thruster of a nano-satellite."

[7] Khuller, Aditya R., et al. "Pulsed plasma thruster for multi-axis cubesat attitude control applications." *2018 Joint Propulsion Conference*. 2018.

[8] O'Reilly, Dillon, Georg Herdrich, and Darren F. Kavanagh. "Electric propulsion methods for small satellites: A review." *Aerospace* 8.1 (2021): 22.

[9] Zhang, Zhe, et al. "A review of the characterization and optimization of ablative pulsed plasma thrusters." *Reviews of Modern Plasma Physics* 3.1 (2019): 1-41.

[10] LING, William Yeong Liang, et al. "A brief review of alternative propellants and requirements for pulsed plasma thrusters in micropropulsion applications." *Chinese Journal of Aeronautics* 33.12 (2020): 2999-3010.

[11] Naidu, Motukuru S. *High voltage engineering*. Tata McGraw-Hill Education, 2013.

[12] Saraf, Gaytri, et al. "High Voltage Dc Generation using Marx Generator." *Ijarcce* 6.5 (2017): 611-645.

[13] Rodriguez, E., et al. "Digitally addressable digital dimming electronic ballast based on CAN bus." *APEC 07-Twenty-Second Annual IEEE Applied Power Electronics Conference and Exposition*. IEEE, 2007.

[14] Nawaz, Anuscheh, et al. "Pulsed plasma thrusters for primary propulsion and attitude control of a small all electrical satellite." *International Space Propulsion Conference, Sardinia, Italy June*. 2004.

[15] Cho, Min Gyoung, and Hong-Gye Sung. "Numerical Modeling of Pulsed Plasma Thruster Performance with Teflon Ablation and Ionization." *International Journal of Aeronautical and Space Sciences* 20.2 (2019): 415-422.

[16] Selstrom, Jeremy J. *Thrust and performance study of micro pulsed plasma thrusters*. Air Force Inst of Tech Wright-Patterson Afb oh School of Engineering and Management, 2010.

[17] Guarducci, F., M. Coletti, and S. B. Gabriel. "Design and testing of a micro pulsed plasma thruster for Cubesat application." *32nd international electric propulsion conference*. 2011.

[18] Palumbo, Dominic J., and Martin Begun. "Plasma acceleration in pulsed ablative arc discharges." *Final Report* (1977).